國 立 交 通 大 學
生物科技研究所
碩士論文

探討霍氏格里蒙菌中熱穩定性溶血素之原始型與突變型生化活性與生物物理特性的差異

Biological and Biophysical Characterization of Wild-type and Mutated Thermostable Direct Hemolysin from *Grimontia hollisae*

研究生：吳宜芳

Student: Yi-Fang Wu

指導教授：吳東昆 博士

Advisor: Prof. Tung-Kung Wu Ph.D

中華民國九十九年七月

探討霍氏格里蒙菌中熱穩定性溶血素之原始型與突變型生化活性與生物物理特性的差異

Biological and Biophysical Characterization of Wild-type and Mutated Thermostable Direct Hemolysin from Grimontia hollisae

研究生：吳宜芳　　Student: Yi-Fang Wu

指導教授：吳東昆 博士　　Advisor: Prof. Tung-Kung Wu Ph.D

國立交通大學

生物科技研究所

碩士論文

A Manuscript of Dissertation
Submitted to Department of Biological Science and Technology
College of Biological Science and Technology
National Chiao Tung University
in partial Fulfillment of the Requirements for
the Degree of Master of Philosophy
in
Biological Science and Technology Hsinchu,
Taiwan, Republic of China

July, 2010

中華民國九十九年七月

中文摘要

熱穩定溶血素（Thermostable direct hemolysin, TDH）在腸炎弧菌中被認為是最主要的毒性因子。霍氏格里蒙菌所產生的熱穩定溶血素已經成功被表現、純化及被定義其生化特性。然而由於我們所取得的菌株（*G. hollisae* BCRC 15890），其所產生的 TDH 與發表在 NCBI 上的 TDH（*G. hollisae* 9041）在其胺基酸序列上有所出入。最主要的差異是位在胺基酸 53, 59 以及 63 號的這三個位置。同時我們也發現兩者在生化特性上有很大的差異，最明顯的就是在 *G. hollisae* BCRC 15890 與 *V. parahaemolyticus* 產生的 TDH 同樣擁有相似的生化性質，而 *G. hollisae* 9041 則否。當蛋白質加熱至 85°C 以上再經快速降溫過程到 4 度時，此蛋白質的溶血活性可以回復至先前未經處理時的百分之八十以上；但當蛋白質加熱在 60°C 與 80°C 之間，快速冷卻後此時的蛋白質卻不具有溶血活性，這一種現象我們稱之為 Arrhenius effect。此效應存在至今已約 100 年，到現在一直無法被解釋為何蛋白質有如此特殊的現象。在這裡我們試圖利用此兩種不同性質的蛋白質來探討令人難以解釋的現象。

首先我們利用分生技術將 53, 59,以及 63 三個位置分別做單點、雙點以及三點突變。包括野生型總共可以獲得八種蛋白質。接著我們利用 DSC 去探討各個蛋白質的相轉變溫度。接著利用 CD 觀察各個蛋白質經由升溫所導致相轉變的過程中其二級結構是如何變化的。最後利用紅血球及 AGS 細胞株觀察各個蛋白質其對溶血以及對細胞的影響。我們獲得的初步結論是，單一點突變的蛋白質會使得蛋白質結構較不穩定，但其依然保有 Arrhenius effect；雙點突變 53 及 59 或 59 及 63 位置會使得蛋白質喪失原本具有 Arrhenius effect 的現象，而三點突變的蛋白質亦會具有相同的結果。而雙點突變在 53 及 63 位置在升溫過程時其二級結構變化會介於具有 Arrhenius effect 蛋白與不具有 Arrhenius effect 蛋白之間。我們認為 Arrhenius effect 的有無關鍵與蛋白質結構的穩定度有一定的關聯性。由 CD 結果得知，擁有 Arrhenius effect 的蛋白質在高溫狀況下其二級結構相較於喪失

Arrhenius effect 蛋白質還要鬆散，所以在經由快速降溫的過程中蛋白質得以重新摺疊成具有溶血功能的構形；在喪失 Arrhenius effect 的蛋白質中我們發現這些蛋白質在加熱 60^{o}C 以上時，其二級結構的構形皆會維持在 α-helix 且其含量不受溫度的影響。我們認為這些蛋白質結構在高溫下並沒有被打開，所以在冷卻後其構形依然維持在 60^{o}C 的纖維化型態(fiber form)。有趣的是，這樣的結果與先前的報導不盡相同。在細胞毒性以及溶血活性方面皆以雙點突變 53 以及 63 最為嚴重。這些蛋白質對於細胞及紅血球有不同程度的傷害性，就先前的研究指出其可能與結合到細胞膜表面上的特定物質有關係或與蛋白質形成四聚體(tetramer)的能力有關係。綜合上結果得知，就 *G. hollisae* TDH 而言，當其 53, 59,及 63 此三個位置經突變效應後，確實在其生化特性或結構方面會受到不同程度的影響。

Abstract

The recombinant thermostable direct hemolysin from *Grimontia hollisae* (*G.h*-rTDH) exhibited an "Arrhenius effect", from which it was detoxified by heating at approximately 60-70^{o}C, but reactivated its functional activity by additional heating above 80^{o}C, coupled with a rapid cooling treatment. In order to characterize this paradoxical phenomenon, we compared the *tdh* gene from the difference species of *Grimontia hollisae* listed in a database and used sequence alignment to identify the critical residues. In addition, we used site-directed mutagenesis to construct the corresponding TDH mutants and obtained various mutated proteins via chromatographic purification. In this study herein, we investigated the individual or collective mutational effect on Tyr53, Thr59, and Ser63 positions of *G.h*-rTDH to characterize the Arrhenius effect, hemolytic activity, and the biophysical properties of various mutants, respectively. In contrast to the *G.h*-rTDH wild-type (*G.h*-rTDH^{WT}) protein, no Arrhenius effect was detected from the *G.h*-rTDH$^{Y53H/T59I}$ and *G.h*-rTDH$^{T59I/S63T}$ double-mutants, as well as the *G.h*-rTDH$^{Y53H/T59I/S63T}$ triple-mutant. These mutants also exhibited a different hemolytic activity compared to that observed for the *G.h*-rTDH^{WT} protein. The differential scanning calorimetry (DSC) results consistently showed that the Arrhenius effect-losing and -retaining mutants exhibited higher and lower endothermic transition temperatures (T_m) than that of the *G.h*-rTDH^{WT}, respectively. Circular dichroism (CD) measurements indicated the partial decrease of β–sheet structures near the endothermic transition temperature, consistent with the conformational change of the Arrhenius effect-losing and -retaining protein. Moreover, we also evaluated its toxic effects by assessing their cytotoxic activities against in AGS cells.

謝誌 (Acknowledgement)

兩年多的日子裡，作息規律而踏實，學業由陌生到瞭解。時光匆匆，很快的碩士生涯結束了，在這裡我學到了老師們以及每位學長姐的經驗與努力。

首先，要先感謝我的指導教授吳東昆老師，感謝老師給我進入實驗室學習的機會，讓我在兩年的碩士生涯裡，收穫良多。並且由衷的感謝老師在百忙之中指導我完成論文以及期間給予最大的幫助與鼓勵，讓我在碩士班期間得以順利完成學業。感謝擔任口試委員的李耀坤老師和廖亦翰老師，感謝您們在百忙之中抽空前來指導學生，因為您的細心審閱以及寶貴的建議讓我的論文更臻完美，感謝您！

而我的實驗之所以能順利的完成，在這一個過程中，必須要誠心地感謝許多參與其中並且不吝給予幫忙的很多人。感謝生科系張家靖老師、學亮學長、虹瑋學妹在 DSC 上給予的幫助與指導。感謝應化系李耀坤老師、黃靜萍博士、貴儀中心李蘊明小姐、在 CD 上給予的協助，讓我得以在最短的時間內順利完成這部分的實驗成果。感謝文亮老師在細胞實驗上給予的協助，謝謝您！

接著，感謝本組最資深以及默默指導我們的裕國學長，感謝您為 TDH 組建立如此深厚的基礎，讓我們得以更快進入狀況，在我們遭遇問題時也與我們共度難關，讓我們的實驗更加順利！感謝默默撐起 TDH 組一片天的聖慈學姊，感謝您總是默默的為我們每一個人付出。您，不論在實驗或在生活上總是給予我很大很大的幫忙；您，在我心中是不可或缺的極重要角色；您的不拘小節以及傳統女性的犧牲奉獻精神是我最佳的生活導師，感謝您！感謝 Milli 學姊，感謝您在英文上給予的協助。感謝幽默又充滿智慧的晏任學長，感謝您在實驗與生活上的照顧與幫忙，感謝您在我低潮時給予的寶貴建議，讓我很快的重新進入正軌，有你真好。感謝俞靜學妹、彥伶學妹、婉婷學妹，感謝你們幫忙分擔 TDH 的繁重工作，謝謝你們。這段期間，追隨學長姐們的步伐，讓我感受到身為研究學者的我們，對於學術應有的熱忱與堅持，有這種感覺，真的很棒！也因為有你們的相伴讓我在實驗上不孤單寂寞。謝謝你們！

感謝程翔學長、媛婷學姐、晉豪學長、晉源學長、文鴻學長，謝謝您們對實驗室以及學弟妹們無私的付出與掏心傾力的指導，因為有你們實驗室才會運作的如次順暢與井然有序，你們真的很重要。非常感謝程翔學長在這期間的照顧與幫忙，感謝您總是給我信心與鼓勵，讓我有繼續向前走的動力，感謝您陪伴我度過了不順遂的實驗生活，感謝有您！感謝天昶學長以及已經畢業的禕婷學姊、亦諄學姊感謝你們在我剛進實驗室時帶領青澀的我認識實驗室，使我能迅速的熟悉並且融入當中。感謝一起奮鬥的同學們，靜婷、書涵、亦齊，謝謝你們常常提醒迷糊又記性不好的我許多事情；謝謝你們陪伴我一起闖關，讓我在求學的路上不那麼孤軍奮戰！感謝學弟妹，怡臻、欣怡、世穎、欣芳、球球、man^2、瑛婷、 孟

兒、欣樺、富生，感謝你們分擔實驗室的雜事，讓我們可以全心全意專注在實驗上，也謝謝你們讓實驗室充滿了歡笑與年輕的活力!感謝依娟學姐、亦榮學長、建成學長、小新學長、阿伯、冠倫和宗翰學弟，感謝您們在實驗上對我的幫忙!

最後，最重要的，我要感謝我的家人，謝謝你們全力支持我做我想做的事情，謝謝你們當我心靈上的避風港，你們總是給我許多許多的溫暖與感動，謝謝你們為我付出那麼多，我愛你們!!

謝謝在這期間支持我、關心我的朋友們，很開心這段回憶中有你們相伴!!

宜芳

2010/07/28

Table of Contents

Table of Figures

Table of Tables


E S A
1896

Chapter 1

General Introduction

1.1. Vibrionaceae family

The Vibrionaceae are a family of Proteobacteria. They are gram-negative organisms and belong to facultative anaerobes, capable of fermentation. The family Vibrionaceae currently comprises six validly published genera: *Aliivibrio*, *Salinivibrio*, *Enterovibrio*, *Grimontia*, *Photobacterium*, and *Vibrio*.

1.1.1 Vibrio species

Many *Vibrio* species are pathogenic to humans and have been implicated in food-borne disease. *Vibrio* infections are more frequently encountered in coastal states, apparently due to the greater consumption of raw or uncooked shellfish. *Vibrio spp.* distinct from *Vibrio cholerae* and *Vibrio mimicus*, do not grow in media that lack added sodium chloride, and are referred to as "halophilic".

The *Vibrio* species with the most medical significance include *Vibrio cholera, Vibrio parahaemolyticus, Vibrio vulnificus*, and *Grimontia hollisae.* Major clinical manifestations of infection by this type of organism include primary septicemia, gastroenteritis, and wound infections[1]. Primary septicemia and gastroenteritis are usually caused by ingesting contaminated seafood. Generally, the symptoms of gastroenteritis include diarrhea, vomiting, and abdominal pain, where antibiotics are needed when infection is present. Moreover, primary septicemia is also a disease of the circulation system, caused by invasion of the bacteria into the blood vessels from hepatic portal vein or the intestinal lymph system. Patients with primary septicemia might have fever, chills, hypotension on presentation, nausea, vomiting, diarrhea,

abdominal pain, and skin lesions[2]. In addition, if injured skin comes into contact with the contaminated marine life or seawater, it could cause wound infections, edema, erythema, and blain.

Table 1. Pathogenic Vibrio species associated with human infections[1].

Species	Gastrointestinal tract	wound	Ear	Primary seoticaemia	Bacteremia	Lung	Meninges
V.cholerae 01	++	(+)	*	*	*	*	*
V.cholerae non-01	++	+	+	(+)	(+)	*	(+)
V. parahaemolyticus	++	+	(+)	*	(+)	(+)	(+)
V. vulnificus	+	++	*	++	+	(+)	(+)
V. fluvialis	++	*	*	*	*	*	*
V. alginolyticus	*	++	+	*	(+)	*	*
V. damesela	*	++	*	*	*	*	*
V. furnissii	(+)	*	*	*	*	*	*
V. hollisae	++	*	*	(+)	*	*	*
V. mimicus	++	+	+	*	*	*	*
V. metschnikovii	(+)	*	*	(+)	*	*	*
V. cincinnatiensis	*	*	*	*	(+)	*	(+)

NOTE : ++, most common site of infection ; +, other sites of infection ; (+), rare sites of infection ; *, infection remains to be firmly establish.

1.1.2 Vibrio parahaemolyticus

V. parahaemolyticus, a common pathogenic bacterium of food-borne gastroenteritis in people, is frequently isolated from a variety of marine organisms consumed as seafood. *V. parahaemolyticus* was first described as the cause of gastroenteritis in Japan, and was first found in the United States by Baross and Liston (1968) in the estuarine waters of Puget Sound[3]. Between 1971 and 1978, *V. parahaemolyticus* was implicated in 14 disease cases via either crab, oyster, shrimp,

and lobster infection, which might be caused by the consumption of raw or insufficiently heated seafood, or by consumption the properly cooked food but still be contaminated after its cooking[4,5]. *V. parahaemolyticus* has a worldwide distribution in estuarine and coastal environments, and has been isolated not only from many species of fish, shellfish, and crustaceans, but also from the cases of gastroenteritis in humans. Among the pathogenic factors, *V. parahaemolyticus* TDH has been considered as a major virulence factor in the case of gastroenteritis[6].

1.1.3 Grimontia hollisae

Grimontia hollisae, a species of Vibrionaceae, which was first described by Hickman et al. and recently reclassified by Thompson et al. causes moderate to severe cases of gastroenteritis including diarrhea and abdominal pains[7,8]. This organism was reported as typically not growing on TCBS agar or MacConkey agar, but does grow well on sheep blood agar and marine agar[8]. *Grimontia hollisae* was found with much greater frequency in samples taken from clinical cases of gastroenteritis, acute diarrhea, bacteremia, and septicemia[9-13]. Although epidemiological evidence[8,9] and the halophilic nature of the vibrio suggested that *G. hollisae* is an organism of marine origin, to the best of our knowledge, the isolation of *G. hollisae* from the marine environment is not the only way for acquisition. Some *Vibrio* species can also cause infections in humans and have been isolated from a variety of intestinal and extra-intestinal sites[14].

1.2 Thermostable direct hemolysin (TDH)

Many important pathogenic factors of *Vibrio*, such as hemolysins, proteases, hemagglutinins, and other hydrolytic exoenzymes, have been reported to contribute to virulence, or to facilitate the disease process[15,16]. Among these factors, hemolysin is

known to be the most fearful virulence factor, which is involved in the gastrointestinal disorders caused by *V. parahaemolyticus*. *V. parahaemolyticus* is commonly isolated from the cases of gastroenteritis in humans, and thermostable direct hemolysin (TDH), has further been considered as a major virulence factor in the cases of gastroenteritis. This protein has been confirmed to contain hemolytic, cytotoxic, enterotoxic, lethal (in mice), and cardiotoxic activities[17].

TDH is a pore-forming toxin of approximately 2 nm in size on erythrocyte membranes and causes colloidal osmotic lysis. TDH consists of 165 amino acid residues to perform a variety of biological activities including hemolytic activity, cytotoxicity, cardiotoxicity, and enterotoxicity. TDH with toxic effects was identified from a variety of *Vibrio* species, including *V. cholera* non-O1, *V. parahaemolyticus*, *V. mimicus*, *V. alginolyticus*, and *G. hollisae*, and was proposed as a major virulence factor of *V. parahaemolyticus*[18]. Although scientists have originally studied its hemolytic properties, TDH has been long suspected to be an enterotoxin involved in most cases of *V. parahaemolyticus* diarrhea. *V. parahaemolyticus* has been recognized as an agent of gastroenteritis associated with the consumption of seafood, but not all strains of this species are considered to be truly pathogenic. An important virulence factor that has been considered in *V. parahaemolyticus* gastroenteritis is TDH. TDH is one putative virulence factor that has been epidemiologically associated with disease, and it is one of the hemolysins produced by *V. parahaemolyticus* that produces beta-type hemolysis on a special blood agar medium, Wagatsuma agar[9,19]. Almost all *V. parahaemolyticus* strains isolated from clinical specimens demonstrated this hemolytic activity, which has been called the Kanagawa phenomenon (KP), only 1-2% of strains from nonclinical sources are KP positive[19,20]. Accordingly, this hemolysin has been considered an important virulence factor, and the KP reaction has thus been used as a marker for virulence detection. TDH causes intestinal fluid

secretion, as well as cytotoxicity in a variety of cell types[21]. The effects of the toxin on human amniotic membrane cells (FL cells) have been characterized by loss of viability and by some morphological changes, including the disappearance of microvilli from the cell surface, degeneration of the cytoplasm, and disintegration of the nucleus[22]. Furthermore, the Ca^{2+}-independent cytotoxicity of TDH in a human embryonic cell line (Int407) was also reported, where it caused damage to plasma membranes and lysosomes, as well as induced a cellular degeneration in the form of large transparent blebs[23]. Although the TDH virulence factor has been studied, the mechanism of virulence responsible for these activities has not been fully elucidated.

TDH is detoxified by aggregation into fibrils, formed after being heated at 60-70 ℃, which can be reversibly refolded into the toxic native form by being rapidly cooled after unfolding at higher temperatures[24]. Transmission electron microscopy further indicates the nature of the fibrillar structure of TDH (TDHi). These fibril formed structures show both the property of the nucleation-dependent elongation, and the fluorescent incensement from its thioflavin T fluorescence. Formation of *β*-rich structures of TDH were also observed in the presence of lipid vesicles containing ganglioside GT1b[25], a putative TDH receptor. Congo red, which is a well-known dye sensitive for detection of amyloid fibrils, was found to inhibit the hemolytic activity of TDH in a dose-dependent manner. These findings support the idea that the conformational change in TDH structure, with the increase in its *β*-sheet content, in a cellular membrane, may be associated with its cytotoxicity[24].

In 1988, it was reported that a vibrio isolated from the intestine of a coastal fish was identified as *G. hollisae* by its biochemical characteristics and by reaction with a gene probe for the thermostable direct hemolysin of *V. parahaemolyticus* (Figure 1). The hemolysin produced by the isolate from the coastal fish had traits identical to those of the thermostable direct hemolysin-like hemolysin produced by a clinical

strain of *G. hollisae*[26] (Figure 1B). The hemolysis characteristics of TDH are fascinating and also thought to be responsible for the virulence of *G. hollisae*. *G. hollisae* has been reported only in clinical cases (largely from diarrheal stools). *G. hollisae* has also been reported to be isolated from the coastal environment. This finding is important in that it presents evidence to support previous suggestions that *G. hollisae* infection originated from ingestion of contaminated food or contact with the environmental reservoir. Recently, patients with severe gastroenteritis and hypovolemic shock symptoms have been identified to be infected with *G. hollisae* and no other enteric pathogens, suggesting a likely underestimation of the incidence of *G. hollisae* infections[2726].

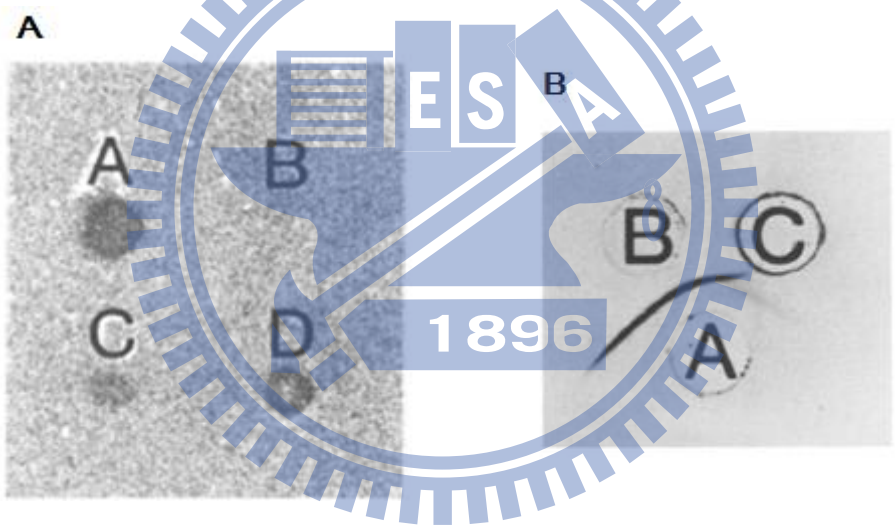

FIGURE 1: (A) DNA hybridization test with the *tdh* gene probe. A: Kanagawa phenomenon-positive *V. parahaemolyticus*; B: Kanagawa phenomenon-negative *V. parahaemolyticus*; C: *G. hollisae* ATCC 33564; D: *G. hollis*ae KUMA871. (B) Ouchterlony immunodiffusion analysis of TDH-like hemolysin produced by *G. hollisae*. A: anti-TDH rabbit serum; B: purified TDH; C: concentrated culture supernatant of *G. hollisae* KUMA871[26].

1.2.1 Arrhenius effect

As early as 1907, staphylococcal alpha-toxin was found to show the Arrhenius effect, and the mechanism of this effect has been studied by several researchers[28]. For staphylococcal alpha-toxin, Arrhenius reported that it was inactivated by heating at 70^{o}C, but was reactivated by heating at 100^{o}C[28]. This phenomenon has been described as the Arrhenius effect, and several workers have studied this Arrhenius effect through the investigation of *staphylococcal* alpha-toxin, proposing the existence of some substance which interacts with alpha-toxin at 60^{o}C[28]. On the other hand, some reports indicated that active alpha-toxin aggregates at 60^{o}C to an insoluble, nontoxic form, whereas at higher temperatures soluble active toxin is released. Crude hemolysin of *V. parahaemolyticus* shows an Arrhenius effect similar to that of staphylococcal alpha-toxin[28-31]. In the thermostable direct hemolysin (TDH), a major virulence factor of *V. parahaemolyticus* is detoxified by heating at approximately 60-70^{o}C, but is reactivated by additional heating above 80^{o}C. This paradoxical phenomenon has been shown in several strains of *V. parahaemolyticus* even though it still remained unexplained for almost 100 years[24]. The previous study demonstrated that the Arrhenius effect in the TDH from *V. parahaemolyticus* is related to structural changes from a soluble form into a fibrils form. The native TDH (TDHn) is transformed into the nontoxic fibrils rich in β-strands by incubation at 60^{o}C (TDHi). The TDHi fibrils are dissociated into unfolded conformations by further heating above 80^{o}C (TDHu). The rapid cooling of TDHu results in the refolding of the protein into the toxic TDHn, whereas the protein is trapped in the TDHi structure by a slow cooling of TDHu (Figure 2). TDHi, with fibrillar structure has no hemolytic activity at 37^{o}C, consistent with the Arrhenius effect. When TDHi fibrils are incubated above 80^{o}C they dissociate into unfolded states, which can further refold into toxic TDHn upon rapid cooling to 37^{o}C (Figure 3). This is an unusual phenomenon because the

formation of inactive protein aggregation is generally irreversible.

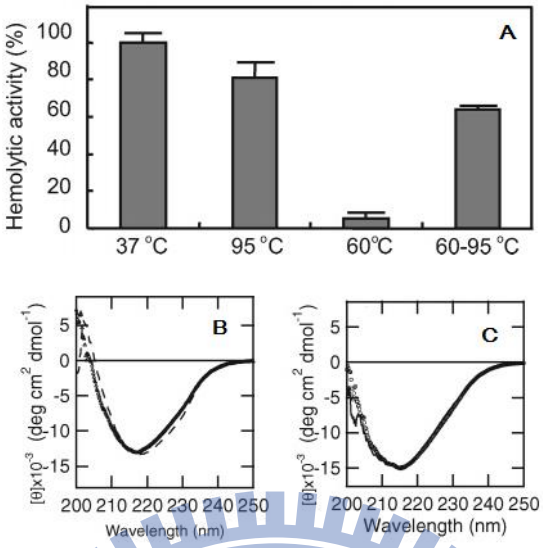

FIGURE 2: Effect of heat treatment on the conformation of TDH. (A) Relative hemolytic activities of TDH, measured at 37℃ after various heat treatments (n = 5 per group) (B) CD spectrum of TDH at 37°C after rapid cooling(Δ). The spectrum is identical to that of TDHn (dashed line). (C) CD spectrum of TDH at 37℃ after slow cooling (O). The spectrum was identical to that of TDHi at 57.5℃ (solid line)[24].

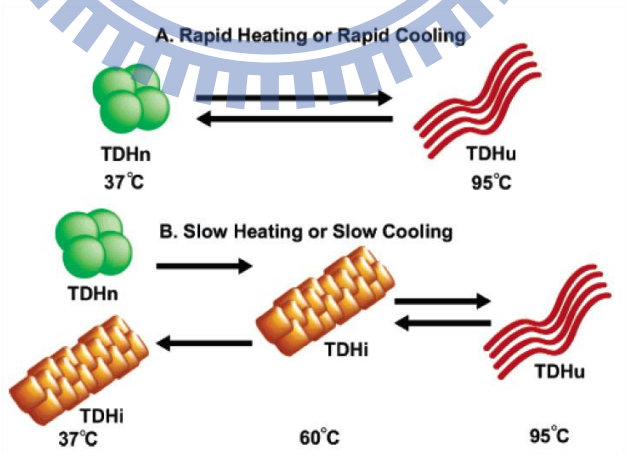

FIGURE 3: Model of heat-induced conformational change of TDH. (A) Rapid heating and cooling. (B) Slow heating and cooling[24].

Chapter 2

Global Research Goals and Design

TDH widely distributed in the strain of *Grimontia hollisae* and a few *Vibrio* species, has a variety of biological activities in animals, including hemolytic activity, cytotoxicity, and enterotoxicity in mice[32]. The information of physiochemical and biophysical properties of *G.h*-rTDH, however, have not been well reported. In this study, we aim to analyze the physiochemical and biophysical characterization of *G.h*-rTDH. First, the *G.h*-rTDH was cloned from a commercial *Grimontia hollisae* strain, BCRC 15890. The amino acid sequence of the cloned *G.h*-rTDH was compared with that of the published *tdh* gene, *Grimontia hollisae* 9041. From the results of sequence alignment, three distinct amino acid changes, *i.e.* Tyr53→His53, Thr59→Ile59, and Ser63→Thr63, between *tdh* gene from *G. hollisae* BCRC 15890 and *G. hollisae* 9041, were observed and examined, attributed with the physiochemical and biophysical characteristics.

As mentioned previously, the TDH of *V. parahaemolyticus* has the ability to revert to a native form via a rapid-cooling treatment after it was unfolded at high temperatures, without any assistance of other enzymes or chemical compounds[24]. *G.h*-rTDH^{WT} also can display the Arrhenius effect, as the protein physiochemical characterization of *V. parahaemolyticus* TDH has revealed. Interestingly the *G.h*-rTDH$^{Y53H/T59I/S63T}$ lost this Arrhenius effect. It is reasonable to speculate on the interesting points between the recovery ability and the protein structure.

The functional analysis of the amino acid residues is the most essential study to characterize the relationship between the protein function and critical amino acids. The thermostability of *G.h*-rTDH might change when mutants are created. In other

words, the substitution of the amino acid residues might influence the secondary structure directly, and further affect its tertiary structure. Otherwise, it might not change the protein conformation but only permit the energy unfavorable for recovery to its native form. Briefly, by analyzing the changes in activity of *G.h*-rTDH$^{Y53A/T59B/S63C}$ (A=Y or H; B=T or I; C=S or T) mutants, the secondary structure and biophysical relationships will be better understood and elucidated.

Previous reports revealed an effect of a particular mutation on TDH from which a mutant toxin of TDH was formed from *V. parahaemolyticus*, R7, which has a single amino acid substitution of serine for glycine 62, constructed to show the deficiency in its hemolytic activity[33]. Thus, in my experimental design, *G.h*-rTDH$^{Y53A/T59B/S63C}$ may be influencing its hemolytic activity and cytotoxicity via mutagenesis effects. In this work herein, we will study the toxic characterization of *G.h*-rTDH^{WT} and *G.h*-rTDH$^{Y53A/T59B/S63C}$ and propose to understand the mechanism of the Arrhenius effect with the strategy shown in Figure 4.

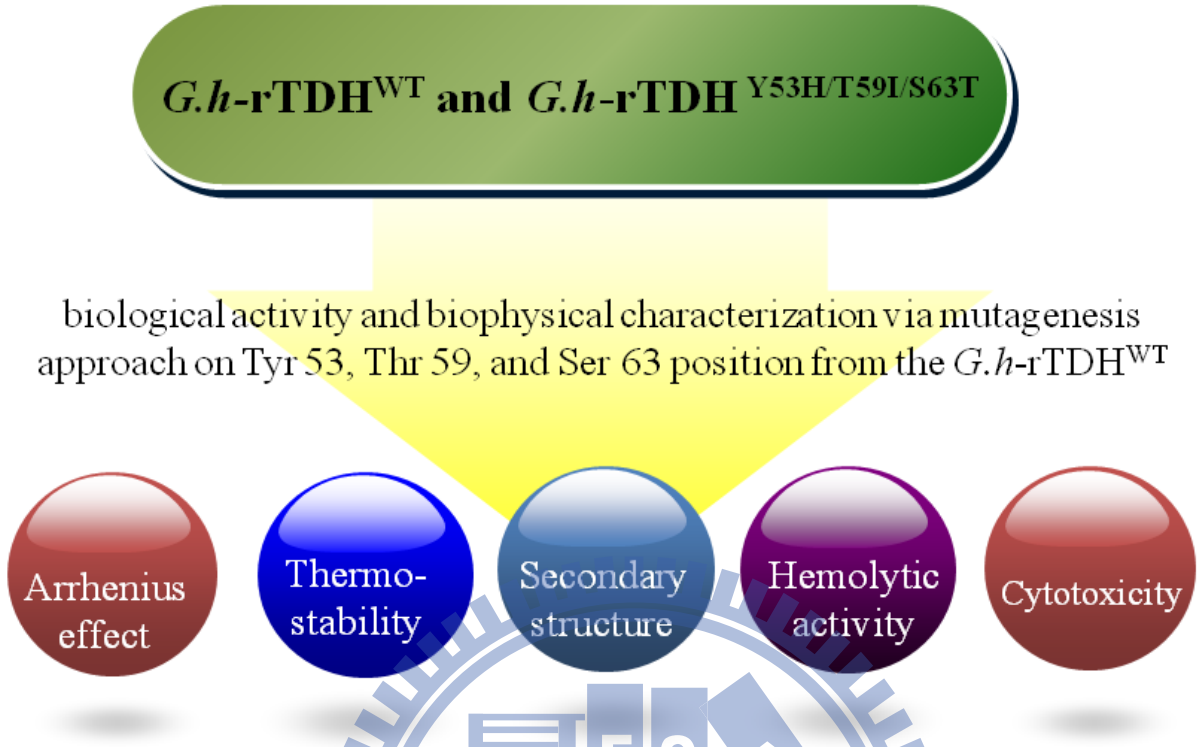

FIGURE 4. The flow chart describes a strategy for analyzing the relationship between protein secondary structure and biophysical characterization when the Tyr53, Thr59, or Ser63 positions of *G.h*-rTDH^{WT} were substituted into various combinations of amino acid substitutions.

Chapter 3

Materials and Methods

3.1 Bacterial strains and materials

Grimontia hollisae (BCRC 15890) was obtained in a freeze-dried form from the Culture Collection and Research Center (CCRC, Hsin-Chu, Taiwan). The bacteria were cultured in a Tryptic Soy Broth (TSB, Difco, Detroit, MI) medium, which was supplemented with 1.5% NaCl and incubated at 37℃ overnight, with shaking (180 cycles/min). This strain showed the hemolytic phenomenon on agar plates containing 5% sheep erythrocytes. Phenyl Sepharose 6 Fast Flow was purchased from Amersham Pharmacia Biotech (Piscataway, NJ, USA).

3.2 Construction, expression, and purification of *Gh*-rTDH^{WT} protein from *G. hollisae*

G. hollisae were cultured in 3 mL Tryptic soy broth (TSB) medium with 3 % sodium chloride (NaCl) at 37^{o}C with continuous shaking for 12 h. Cultures were harvested by centrifugation at 10,000 x g for 1 min at room temperature. The supernatant was removed and the genomic DNA was extracted from the pellets using QIAamp DNA Mini Kit, following the manufacturer's protocol (Qiagen). According to the information derived from the database from National Center for Biotechnology Information (NCBI, http://www.ncbi.nlm.nih.gov) databases, the *tdh* gene was cloned from the *Grimontia hollisae* strain with two primers. The PCR conditions were similar to the general protocol previously published by our research group (Table 2)[34]. The amplified DNA fragment was cloned into pCR® 2.1-TOPO® (Invitrogen) vectors, and the full-length sequence was determined by using an ABI PRISM 3100

autosequencer, according to the manufacturer's protocol (Applied Biosystems, Foster City, CA). A recombinant plasmid harboring the *tdh* gene was transformed into *Escherichia coli* BL21 (DE3) (pLys S) cells by heat shock. Transformants were cultivated at 37℃ with rotary shaking in Luria-Bertani Broth (Difco) supplemented with 50 μg/mL kanamycin, and the culture was incubated for another 16 h. The cells were then harvested by centrifugation at 6,000 x g for 30 min, and resuspended in 15 mL of 20 mM Tris-HCl buffer (pH 7.0). The mixture was sonicated, and the cell debris was removed by centrifugation at 12,000 x g for 30 min at 4℃. Then the crude protein solution was loaded onto a Phenyl-Sepharose 6 Fast Flow column prequilibrated with 20 mM Tris-HCl buffer (pH 7.0) and eluted with a linear 0% to 50% ethylene glycol gradient. Fractions exhibiting *G.h*-rTDH activity were pooled, and added with NaCl to 200 mM concentration. The *G.h*-rTDH was again applied to a Phenyl-Sepharose 6 Fast Flow column with 20 mM Tris-HCl buffer (pH 7.0) containing 200 mM NaCl and then eluted with 4-fold volumes of a step gradient consisting of 200, 100, 50 and 20 mM NaCl in 20 mM Tris-HCl (pH 7.0), respectively, and sole equilibrating buffer without any salt concentration. Pure protein eluted with 20 mM Tris-HCl buffer (pH 7.0). Then, TDH protein was dialyzed against 10 mM phosphate-buffered saline buffer (PBS, pH 7.0) overnight for a hemolytic activity assay.

Table 2. Sequences of PCR primers and PCR condition for PCR amplification of *tdh* gene.

Gene *G. hollisae* (BCRC 15890)	PCR primer sequence[34]
tdh	F 5'- ATGAAATACAGACATCT -3' R 5'- TTATTGTTGAGATTCAC -3'

PCR Condition[34]

	Temperature (^{o}C)	Time	
Denaturation	94 ^{o}C	5 min	
Denaturation	94 ^{o}C	15 sec	35 cycles
Annealing	58℃	1 min	
Extension	72℃	1 min	
Extension	72℃	10 min	

3.3 Construction, expression, and purification of mutant G.h-rTDH$^{Y53A/T59B/S63C}$ protein from *G. hollisae*

The mutant *G.h*-rTDH$^{Y53A/T59B/S63C}$ was constructed by site-directed mutagenesis, using the recombinant plasmid harboring the *tdh* gene as template (*tdh* gene in pCR® 2.1-TOPO®) and using two primers. The PCR condition, purification, and expression method of the mutant *G.h*-rTDH$^{Y53A/T59B/S63C}$ protein were the same as that for *G.h*-rTDH^{WT} (Table 2). The primers for construction of mutant *G.h*-rTDH$^{Y53A/T59B/S63C}$ plasmid are shown in Table 3.

Table 3. The primers sequence for construct of *G.h*-rTDH$^{Y53A/T59B/S63C}$ plasmid

tdh gene	tempelate (*tdh* gene in pCR® 2.1-TOPO®)	PCR primer sequence
tdh^{Y53H}	*tdh*^{WT}	F 5'-GTAAAACGACGGCCAG-3' (M13 forward primer) R 5'-AAAgATgTTCACggACAATCAgTCTTCACA-3'
tdh^{T59I}	*tdh*$^{Y53H/T59I}$	F 5'-GTAAAACGACGGCCAG-3' (M13 forward primer) R 5'-TACAAAgATgTTTATggACAATCAgTCTTCACA-3'
tdh^{S63T}	*tdh*$^{Y53H/S63T}$	F 5'-GTAAAACGACGGCCAG-3' (M13 forward primer) R 5'-TACAAAgATgTTTATggACAATCAgTCTTCACA-3'
tdh$^{Y53H/T59I}$	*tdh*$^{Y53H/T59I/S63T}$	F 5'-GTAAAACGACGGCCAG-3' (M13 forward primer) R 5'-ATAACgTCAggTTCTAAATggTTAACATCC-3'
tdh$^{Y53H/S63T}$	*tdh*$^{Y53H/T59I/S63T}$	F 5'-GTAAAACGACGGCCAG-3' (M13 forward primer) R 5'-ggACAATCAgTCTTCACAACgTCAggTACT-3'
tdh$^{T59I/S63T}$	*tdh*^{WT}	F 5'-GTAAAACGACGGCCAG-3' (M13 forward primer) R 5'-ggACAATCAgTCTTCATAACgTCAggTACTAAA-3'
tdh$^{Y53H/T59I/S63T}$	*tdh*^{Y53H}	F 5'-GTAAAACGACGGCCAG-3' (M13 forward primer) R 5'-ggACAATCAgTCTTCATAACgTCAggTACTAAA-3'

3.4 Assay of hemolytic activity

Hemolytic activity was determined on the human erythrocytes. Human erythrocytes were first washed with 100 mM PBS buffer (pH 7.0) 3 times, and then resuspended to a final concentration of 4% (v/v) in PBS buffer. For the hemolytic activity assay, 0.1 mL of 0.1% Triton X-100, which caused complete release of hemoglobin from erythrocytes and resulted absorbance change at 570 nm, was used as a positive control. Aliquots of 0.1 mL of 100 mM PBS buffer (pH 7.0) were used as negative controls. Different concentrations of the protein solution (0.1 mL) were added to the solution of human erythrocytes (0.1 mL). After incubation at 37℃ for 1 h, the reaction mixtures were centrifuged at 800 x g for 5 min, and the 0.1 mL supernatant was packed. The amount of hemoglobin released from the disrupted erythrocytes was quantified by spectrophotometry on an ELISA reader at 540 nm. The 100% hemolysis activity was defined as the 570 nm absorption, with the hemoglobin released from erythrocytes treated with 0.1% Triton X-100. The equation for hemolytic activity assay is as follows:

Hemolytic activity (%) =

(protein O.D$_{570}$ value – negative value)/(positive value – negative value) x 100

In parallel, the *G.h*-rTDH was subjected to 10% native polyacrylamide gel electrophoresis, and then embedded onto the agar plate containing 5% sheep erythrocytes. The blood agar plate was incubated at 37℃ for an appropriate amount of time to visualize a suitable signal. In addition, *G.h*-rTDH proteins were also electrophoresed on a 15% SDS-PAGE and stained with Coomassie brilliant blue for comparison of the size and homogeneity during the purification process.

3.5 Analyze thermostability of the *G.h*-rTDH protein

The effect of temperature on hemolytic activity of purified *G.h*-rTDH was determined by incubating 1 μM of the purified protein in 0.1 M PBS buffer (pH 7.0) for 30 min at different temperatures (4℃, 16℃, 25℃, 30℃, 37℃, 45℃, 50℃, 55℃, 60℃, 65℃, 70℃, 75℃, 80℃, 85℃, 90℃, 95℃ and 100℃), and then assayed for residual hemolytic activity on 4% human erythrocytes. The hemolytic activity assay method and the equation were described in section.3.4.

3.6 Compare hemolytic activity for *G.h*-rTDH$^{Y53A/T59B/S63C}$

The *G.h*-rTDH$^{Y53A/T59B/S63C}$ mutant was prepared at 200 μg/mL by the described xpression and purification method in section 3.3. A dilution series of protein with half concentration dilutions were incubated with 0.1 mL of 4% human erythrocytes at 37℃ for 1 h. After centrifugation at 3,000 rpm for 5 min, the supernatant was measured at 570 nm. The hemolytic activity assay method and the equation were described in section 3.4.

3.7 MALDI-TOF-TOF MS analysis

The SDS-PAGE band corresponding to *G.h*-rTDH^{WT} was subjected to in-gel trypsin digestion. The in-gel trypsin digestion experiment, excision of protein bands from polyacrylamide gels and the gel particles were prepared for in-gel digestion and washed with 50 μL wash buffer (10mM NH_4HCO_3, 50% ACN) for 15 min. All remaining liquid was removed, and 100 μL ACN was added to cover the gel particles for 20 min. When the gels shrink and stick together, 3 μL of trypsin (20 ng/mL) was added to the gel and incubated for 1 h at 4°C, and then incubated at 37°C overnight. The reaction was stopped with 1% TFA, and 10 min sonication, supernatant recovered, then the sample was directly mixed with MALDI matrix (CHCA, 20 mg/mL in 50%

ACN, 0.1% TFA), and analyzed using an autoflex III (BRUKER). After a default calibration, all MS spectra were recorded in positive reflector mode within a mass range of m/z 500–4000. For an initial MS scan, 4 subspectra with 200 shots per subspectrum were accumulated for each spot using a random search pattern. Spectral peaks were included in the acquisition list for the MS/ MS run of the result-dependent experiment, if they met threshold criteria (S/N above 6). For MS/MS experiments, 2,000 shots per spectrum were accumulated. Subsequently, all acquired MS/MS spectra were searched against the Swiss-Prot database using the MASCOT search engine (biotools, v3.1)**.** Search parameters for peptide and MS/MS mass tolerance were 100 ppm and 100 ppm, respectively, with the allowance for one missed cleavage made from the trypsin digest. The search mode was carried out to identify the variable modification of oxidation (M), and Carboxymethyl (C) groups at the C terminus. Proteins were identified by PMF and MS/MS with MASCOT, which corresponds to $p<0.05$.

3.8 Difference scanning calorimetry (DSC)

DSC measurements were performed using the DSC-Q10 (TA instruments). The DSC-Q10 was run without feedback and 10 min equilibration times at 25^{o}C were used as previously described. The protein was scanned from 25^{o}C to 95^{o}C at a heating rate of 0.5 ^{o}C/min. A pan containing 10 mM Kpi buffer, pH 7.0 was used as a reference. The sample and reference cells of optical operational volume of 0.5 mL were used. Protein samples were concentrated to 0.36 mg/mL in 10 mM Kpi buffer (K_2HPO_4, pH 7.0). DSC data were corrected for instrument baselines and normalized for scan rate and protein concentration. Data obtained for TDH protein were analyzed with the TA advantage specialty Lib program.

3.9 Circular dichroism (CD) spectroscopy

Circular dichroism (CD) spectra were recorded with a J-815 spectropolarimeter (JASCO, Tokyo, Japan) equipped with a thermoelectric temperature controller. Data were processed with software provided by JASCO. Measurements were taken in a quartz cuvette with a path length of 1 mm, and scanned in the interval of 0.2 nm at a rate of 50 nm/min. The data from 6 individual replicates were averaged. The protein concentration was 0.18 mg/mL in 10 mM Kpi buffer (pH 7.0) for the measurement of far-UV (190-250 nm) CD spectrum. The experimental temperatures were 37℃, 50-60℃, 70℃, 75℃, 80℃, 85℃, 90℃, 95℃, and its T_m value, respectively (the T_m value was determined from DSC data). Before measurement, the sample was pre-equilibrated at each experimental temperature for 5 min. The mean residue ellipticity, [Θ], was calculated by using the following relationship:

$$[\Theta]_{MRW} = [\Theta] / (10 \times Cr \times l)$$

Cr is the mean residue molar concentration

l is the cell path in cm

$$Cr = (n \times 1000 \times cg) / Mr$$

n is the number of peptide bonds (residue)

cg is macromolecule concentration (g / mL)

Mr is the molecular weight of species (KDa)

[Θ] was expressed in degrees squared centimeters per decimole.

3.10 Cell line

The AGS cell line (BCRC 60102) is a human stomach adenocarcinoma cell taken from a 54-year-old female Caucasian. Cells were maintained in RPMI Nutrient Mixture (Gibco) supplemented with fetal calf serum (10%, v/v, Gibco) and penicillin streptomycin (1%, v/v, Gibco). Cells were incubated at 37℃ in an incubator of 5%

CO_2 in air. Every 2 to 3 days the culture medium was renewed, and doubling time of this cell line was 20 h.

3.11 Morphology examination

The AGS cells were first cultured in a 6-well plate overnight. Before examination, 100 mM PBS buffer (pH7.0) was used to wash the cells twice, then cells were mixed with 10 g/mL *G.h*-rTDH in RPMI complete medium for 30 min at 26^{o}C. Subsequently, the images of the cell morphology were recorded with the 200x magnification by an Olympus digtal camera.

3.12 MTT assay

For cytoviability, the MTT assay has been widely used as a colorimetric assay for measuring the activity of mitochondrial dehydrogenase that reduce MTT, a tetrazolium dye: 3-(4,5-dimethylthiazol-2-yl)-2,5-diphenyltetrazolium bromide, substrate to form formazan, which is generated only by living cells but not dead cells. In this assay, AGS cells were inoculated in 200 uL of complete growth medium at a concentration of 2 x 10^4 cells in a 96-well microtiter plates. Plates were incubated for 24 h at 37^{o}C in an atmosphere of 5% CO_2 in air. Different concentrations of *G.h*-rTDH were added and treated for 1 h before the supernatant was removed via a centrifugation separation. Fresh MTT solution (5 mg/mL) was dissolved in PBS and filtered by a 0.22 filter, and was diluted 10-fold in a complete medium. A 100 ul aliquot of the above solution was added to each well. Plates were wrapped by the aluminum foil and incubated for a further 5 h at 37 ^{o}C. MTT was then removed from the wells, and the formazan crystals were dissolved in 200 ul of Dimethyl sulfoxide (DMSO). After 10 min, the plate sample absorbance was recorded on a microplate reader (American Bio-Tek) at 570 nm. Assays were performed in three independent

experiments.

3.13 Thioflavin T florescence assay

Thioflavin T (ThT) is a benzothiazole compound that possesses the light-emitting component of leuciferin. It can be utilized to visualize the amyloid beta content of protein in the solution. ThT binds to amyloid fibrils and the florescence intensity can identify the fibril content by florescence spectra. A 10 μg sample of *G.h*-rTDH protein was respectively and sequentially heated to 37^{o}C, 70^{o}C and 90^{o}C for 15 min and then subjected to rapid cooling in ice water for 15 min.

Before measuring the florescence of the fibril content in the solution, ThT and Tris-HCl buffer were premixed. The ThT/Tris solution was as described: ThT powder was dissolved in distilled water and the final concentration was 1 mg/mL (3.14 mM). Then, 1.6 μl of ThT solution was added to 1 mL 50mM Tris-HCl, pH7.0 buffer. Before measurement, an aliquot of 200 μl ThT/Tris solution was mixed with thermally pre-treated protein, the fiber forming protein containing beta sheets became immediately bound to ThT. The florescence of Thioflain T was measured at 460-600 nm when excited at 450 nm using fluorescence spectrophotometry (Hitachi, F-7000). The Thioflavin T was obtained from Sigma (St. Louis, MO).

Chapter 4

Results

4.1 Cloning, sequence analysis and identification of the *G. hollisae tdh* gene

The nucleic acid sequences of *tdh* gene from various *Vibrio* species were aligned and analyzed to find the highly conserved sequences. The primers for the conserved gene were thus designed, and used in the polymerase chain reaction (PCR) to amplify the putative *tdh* gene from *G. hollisae* BCRC 15890 genomic DNA. The construct plasmid carry out *tdh*-mutated gene was obtained from the lab. The PCR amplified *G. hollisae tdh* gene is 570-bp in size and encodes a polypeptide of 189 amino acids involving a signal peptide with 24 amino acids in the *N*-terminal region, and a mature protein of 165 residues, with a predicted molecular mass of 18,616.9 Da. Notably, three distinct amino acid changes, *i.e.*, Tyr53→His53, Thr59→Ile59, and Ser63→Thr63, were observed from the sequence alignment between the PCR amplified *tdh* gene from *G. hollisae* BCRC 15890 genomic DNA (assigned as *G.h*-rTDH^{WT}) and the historically published *tdh* gene from *G. hollisae* 9041 in the NCBI data bank (assigned as *G.h*-rTDH$^{Y53H/T59I/S63T}$). Amino acids sequence alignment between the two *tdh* genes is shown in Figure 5.

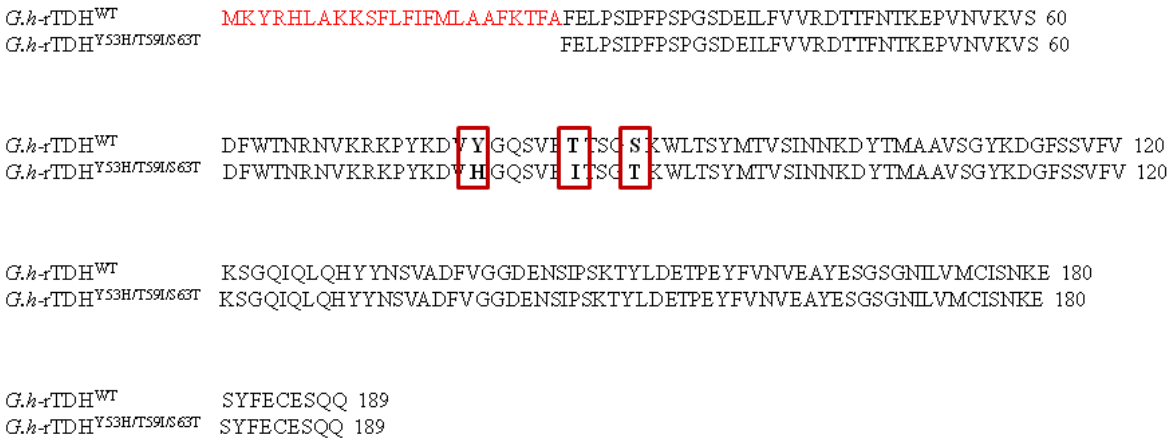

FIGURE 5. The sequence alignment of putative *tdh* genes between the PCR amplicon *tdh* gene from *G. hollisae* BCRC 15890 genomic DNA (assigned as *G.h*-rTDH^{WT}) and the historically published *tdh* gene, from *G. hollisae* 9041 as described in the NCBI data bank (assigned as *G.h*-rTDH$^{Y53H/T59I/S63T}$). The sequence of the signal peptide with 24 amino acids in the N-terminal is shown in red. The distinct amino acid change between *G.h*-rTDH^{WT} and *G.h*-rTDH$^{Y53H/T59I/S63T}$ are red boxed.

4.2 Expression, purification, determination and hemolytic activity of *G.h*-rTDH^{WT}

The wild type *G. hollisae tdh* gene *G.h*-rTDH^{WT} was cloned into the plasmid pCR® 2.1-TOPO® and subsequently transformed into *Escherichia coli* BL21(DE3)(pLysS) cells for protein expression. Following the incubation for 16 h at 37°C, the harvested cells were sonicated for the expressed protein purification using a Phenyl-Sepharose 6 Fast Flow column. After the first round of chromatographic purification for the separation of impurities from crude extraction, the homogenous protein with a molecular mass of approximately 22 kDa, as resolved by 15% SDS-PAGE was collected from the subsequent purification on the same Phenyl-Sepharose 6 Fast Flow column (Figure 6). A single band at approximately 90

kDa was observed by 10% native-PAGE, and the hemolytic activity of this protein band suggested that it is an active tetrameric protein under physiological conditions (Figure 6). MALDI-TOF MS spectrum of peptide mapping via a trypsin digestion further confirmed the identity of *G. hollisae* TDH.

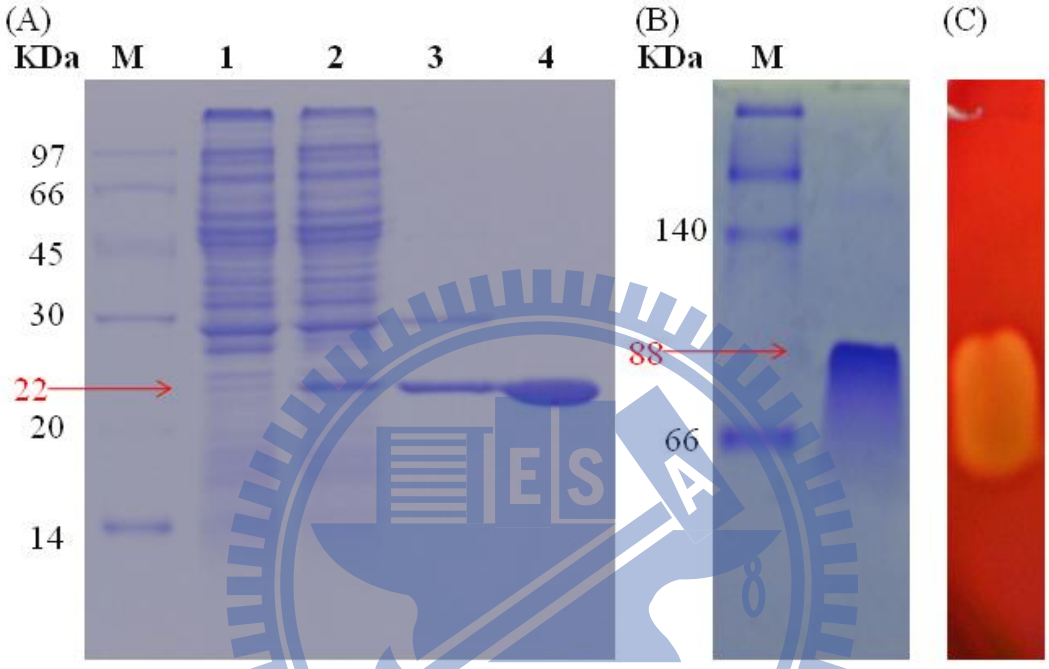

FIGURE 6. Purification and characterization of the *G.h*-rTDH^{WT} protein from *G. hollisae*. (A) The crude protein without *tdh* gene insertion in a pCR® 2.1® -TOPO plasmid was obtained in the BL21(DE3)pLysS strain (lane 1). The crude protein containing the expressed *G.h*-rTDH^{WT} in the BL21(DE3)pLysS strain was also included (lane 2). The homogenous protein with a molecular mass of ~22 kDa was obtained via two Phenyl Sepharose 6 Fast Flow chromatography runs (lane 3 and lane 4). (B) Native-PAGE of purified *G.h*-rTDH^{WT}, with a molecular mass of ~90 kDa. (C) Hemolytic activity of *G.h*-rTDH^{WT}.

4.3 Identification of *G.h*-rTDH^{WT} by MALDI-TOF-TOF MS spectrometry

The purified protein was then subjected to a MALDI-TOF MS spectrometry for the internal amino acid determination to confirm the identity of purified protein. The SDS-PAGE band corresponding to *G.h*-rTDH^{WT} was first applied to an in-gel trypsin digestion as described by Rosenfeld *et al.*[35]. The cutting sites of trypsin are lysine (Lys, K) and arginine (Arg, R), respectively. After digestion, the resulting peptide mixtures were analyzed by MALDI-TOF MS. Among these peptide fragments shown in Figure 7, via a database search for the mass spectrum of the peptide and its fragment ions, the tandem mass spectrum of mono-charged precursor was observed at m/z 1024.543, 1365.788, 1690.949, 2346.302, 2953.530. Following the analysis of the highest signal by MS/MS, the sequence of this fragmental was determined to be ^{35}VSDFWTNR^{42} of *G. hollisae* TDH.

(A)

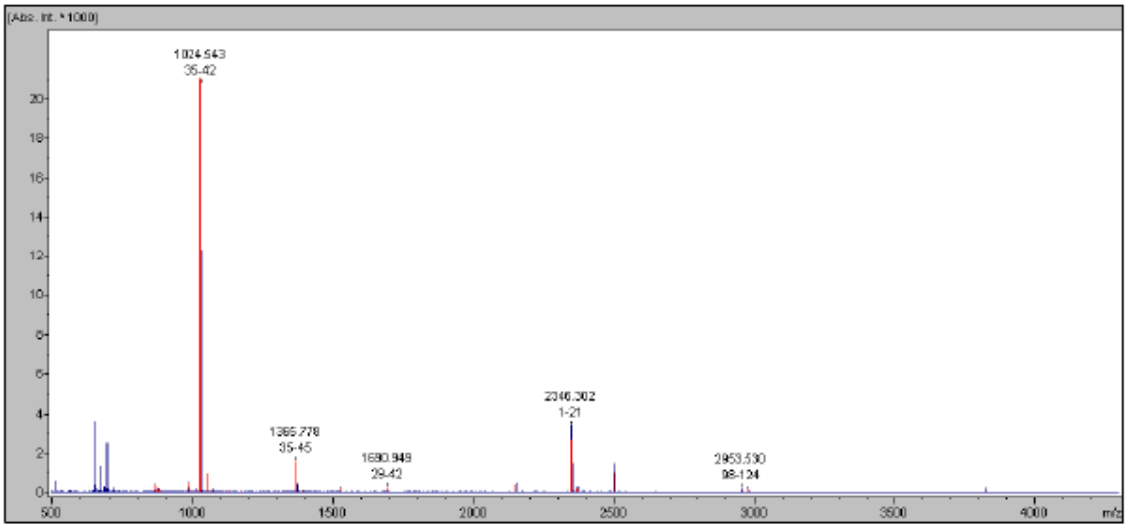

(B)

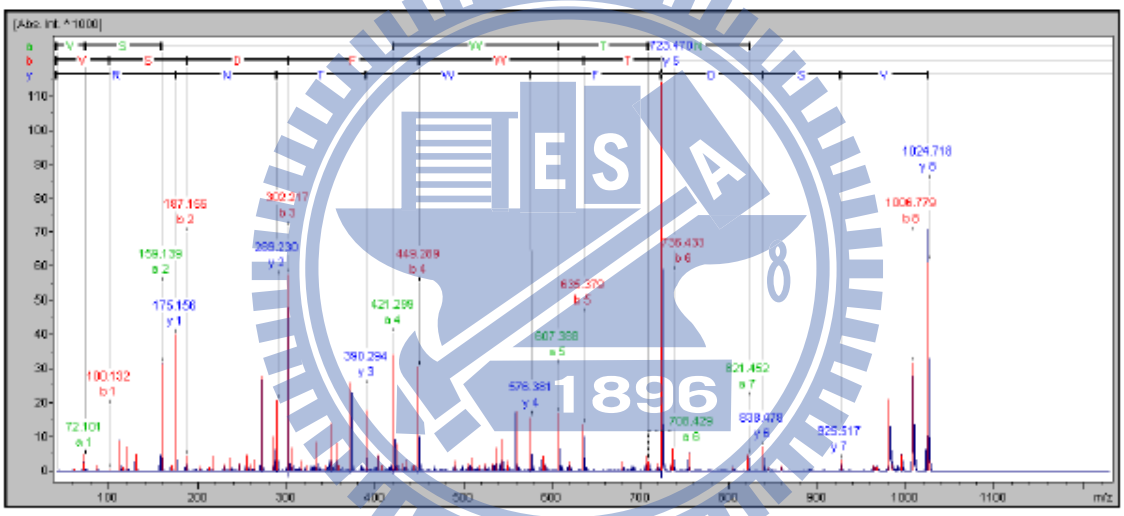

FIGURE 7. (A) MALDI-TOF-TOF MS spectrum and peptide mapping of *G.h*-rTDH protein. (B) Tandem mass spectrum of a signal charged tryptic peptide at m/z 1024.543, was deduced from the mass differences in the y-fragment ion series and partial b-ion and a-ion.

4.4 Expression, purification, and hemolytic activity determination of mutated *G.h*-rTDH$^{Y53A/T59B/S63C}$

In order to understand the role of these distinct amino acid changes between the *tdh* gene from the *G. hollisae* BCRC 15890 strain, and the historically published *tdh* gene from NCBI data bank from *G. hollisae* 9041, seven *G.h*-rTDH mutants specific for different combinations of Tyr53, Thr59, or Ser 63 positions were constructed and purified. The procedures for expression, purification, identification, and hemolytic activity assays of these *G.h*-rTDH$^{Y53A/T59B/S63C}$ mutants were identical with that of Gh-rTDH^{WT}. These seven *G.h*-rTDH$^{Y53A/T59B/S63C}$ mutants include *G.h*-rTDH^{Y53H}, *G.h*-rTDH^{T59I}, *G.h*-rTDH^{S63T}, *G.h*-rTDH$^{Y53H/T59I}$, *G.h*-rTDH$^{Y53H/S63T}$, *G.h*-rTDH $^{T59I/S63T}$, and *G.h*-rTDH$^{Y53H/T59I/S63T}$. As shown in the 15% SDS-PAGE data, all mutated *G.h*-rTDH$^{Y53A/T59B/S63C}$ exhibited a homology protein of approximately 22 KDa. The native-PAGE coupled with the blood agar plate assay further indicated that the corresponding protein bands with molecular mass of ~90KDa possess the hemolytic activity among these *G.h*-rTDH$^{Y53A/T59B/S63C}$ mutants.

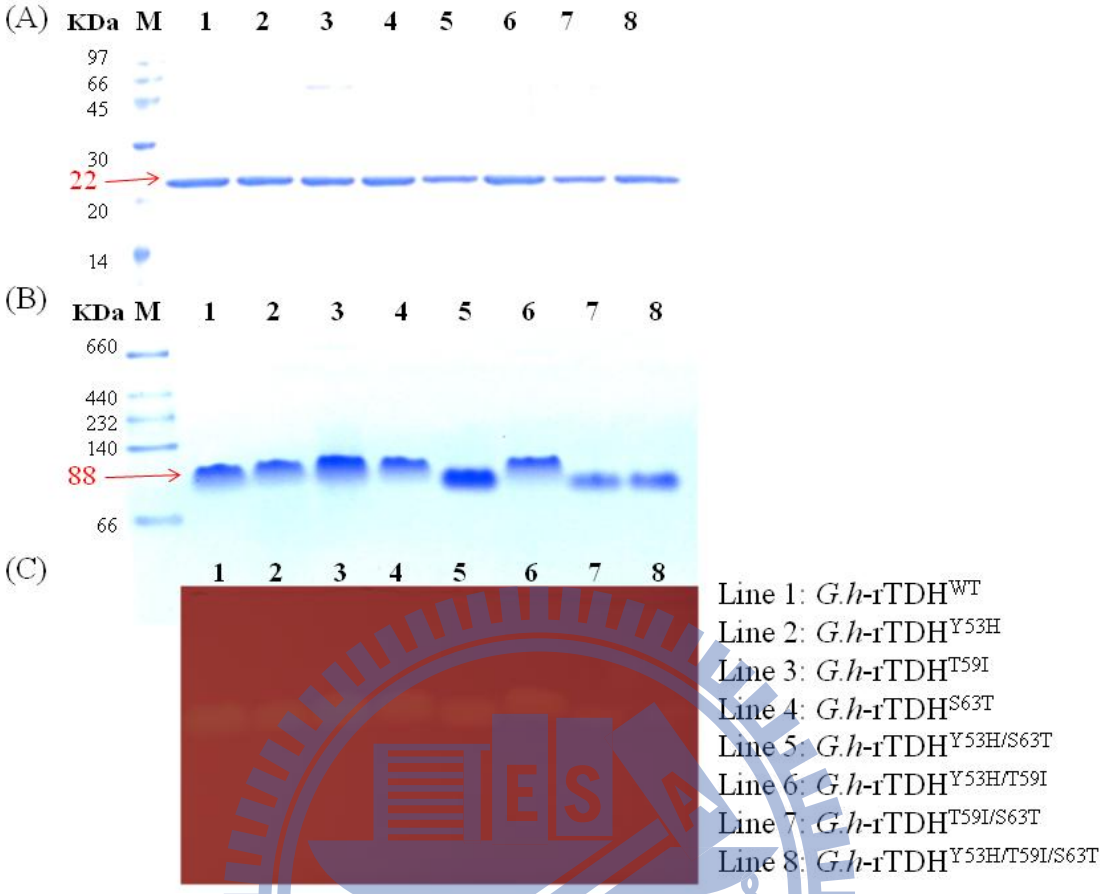

FIGURE 8. (A) SDS-PAGE of purified *G.h*-rTDH with a molecular mass of ~22 kDa from various *G.h*-rTDH mutants. (B) Native PAGE of *G.h*-rTDH mutants, with a molecular mass of ~90 kDa. (C) Hemolytic activity determination of purified *G.h*-rTDH mutants on a blood agar plate.

4.5 The temperature-dependent hemolytic activity analysis and thermostability studies of *G.h*-rTDH^{WT} and *G.h*-rTDH$^{Y53H/T59I/S63T}$

To investigate the thermostability and optimal temperature for hemolytic activity of purified *G.h*-rTDH^{WT} and *G.h*-rTDH$^{Y53H/T59I/S63T}$, a suspension of 5% human erythrocytes was incubated with *G.h*-rTDH protein for 1 h at different temperatures ranging from 4.0-100^{o}C (Figure 9). Interestingly, the hemolytic activity of *G.h*-rTDH^{WT} on human erythrocytes exhibited a common Arrhenius phenomenon, where it lost its activity after a heating under 60-80^{o}C but it reactivated its function by

additional heating over 85°C coupled with a rapid cooling treatment. Under incubation below 55 °C for 30 min, the *G.h*-rTDH^{WT} protein still retained over 80% of its full activity (Figure 9 (A)). In comparison, the *G.h*-rTDH$^{Y53H/T59I/S63T}$ lost the entire hemolytic activity via a heating above 60°C, and no recovering activity was observed after a rapid cooling treatment (Figure 9 (B)).

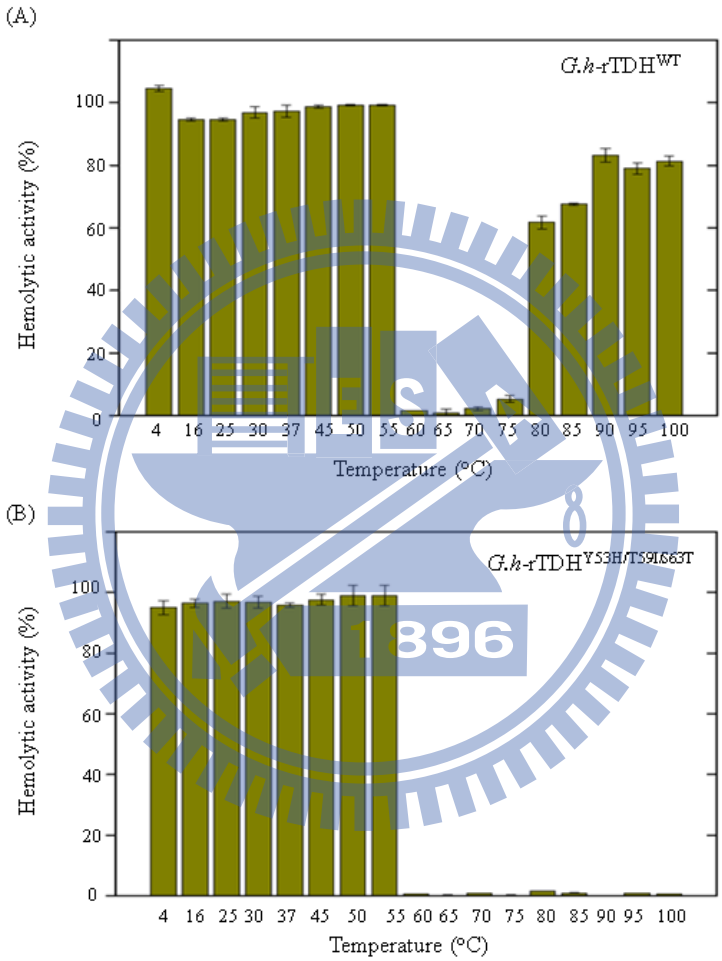

FIGURE 9. Thermostability assay of *G.h*-rTDH^{WT} and *G.h*-rTDH$^{Y53H/T59I/S63T}$ mutants. The relative hemolytic activities were measured at 37°C under various temperature treatments. According to the results, *G.h*-rTDH^{WT} has the Arrhenius effect, whereas the *G.h*-rTDH$^{Y53H/T59I/S63T}$ did not. Data are presented as the means for triplicate experiments. Error bars represent the standard deviations (SD)

4.6 Comparison of hemolytic activity for *G.h*-rTDH$^{Y53A/T59B/S63C}$

In order to investigate the biophysical characterization of various combination mutants on Tyr53, Thr59, or Ser63 positions of *G.h*-rTDH, the hemolytic activity of various mutants on human erythrocytes were further studied. In Figure 10, the hemolytic activities of various *G.h*-rTDH$^{Y53A/T59B/S63C}$ mutants were examined on a 96 well plate. Decreased hemolytic activities were displayed from *G.h*-rTDH$^{Y53H/T59I}$, *G.h*-rTDH$^{T59I/S63T}$, and *G.h*-rTDH$^{Y53H/T59I/S63T}$ mutants. Moreover, the *G.h*-rTDH$^{Y53H/S63T}$ mutant showed more dominant hemolytic activity than that observed for *G.h*-rTDH^{WT}. The hemolysis ability of *G.h*-rTDH^{S63T} and *G.h*-rTDH^{T59I} mutants were very similar, and also more dominant than that observed for *G.h*-rTDH^{WT}. The concentration of various *G.h*-rTDH$^{Y53A/T59B/S63C}$ higher 25 μg/mL caused 100% hemolysis, while lower than 0.39 μg/mL, their hemolytic activity was below the detectable level and had no effect on human erythrocytes.

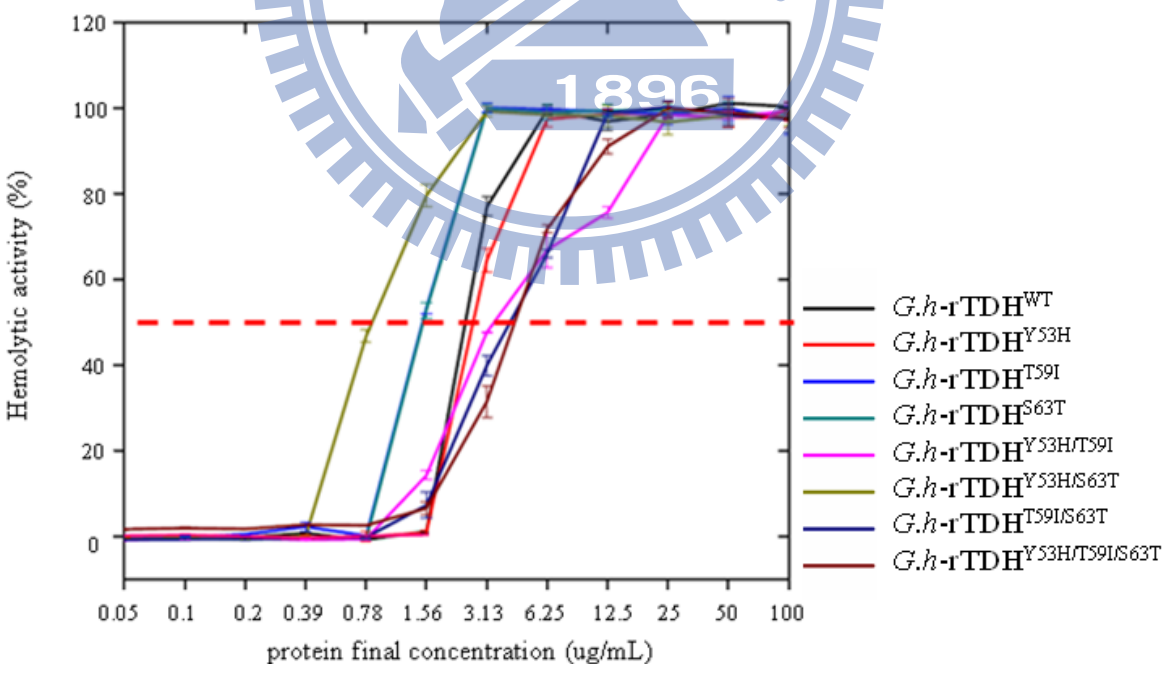

FIGURE 10. Compare hemolytic activity for various *G.h*-rTDH$^{Y53A/T59B/S63C}$ mutant. Data are presented as the means of triplicate experiments. Error bars represent standard deviations (SD).

4.7 Comparison of the hemolytic activity of *G.h*-rTDH$^{Y53A/T59B/S63C}$ mutants at 37^{o}C, 70^{o}C, 90 ^{o}C

As illustrated above, the *G.h*-rTDH^{WT} lost its hemolytic activity under 60-80 ^{o}C but recovered its function via continuing to heat at 90^{o}C coupled with a rapid cooling. This paradoxical phenomenon is referred to as "Arrhenius effect". *G.h*-rTDH^{WT} was first treated with different temperature heating conditions at 37^{o}C, 70^{o}C, or 90^{o}C, coupled by a rapid cooling treatment, respectively. The protein structure or its biophysical characteristics were changed via these three various pretreatments with different significance. The protein structure was changed from a native form into a fiber form, then transformed to the unfold state, and recovered it to its native form via a induced cooling treatment. This conformational change may affect the biophysical properties. Some mutants, *G.h*-rTDH^{Y53H}, *G.h*-rTDH^{T59I}, *G.h*-rTDH^{S63T}, *G.h*-rTDH$^{Y53H/S63T}$, also exhibited this unusual phenomena, but the *G.h*-rTDH$^{Y53H/T59I}$, and *G.h*-rTDH$^{T59I/S63T}$, as well as *G.h*-rTDH$^{Y53H/T59I/S63T}$ lost this Arrhenius effect, even with the concentration elevated to 10 μg/mL (Figure 11).

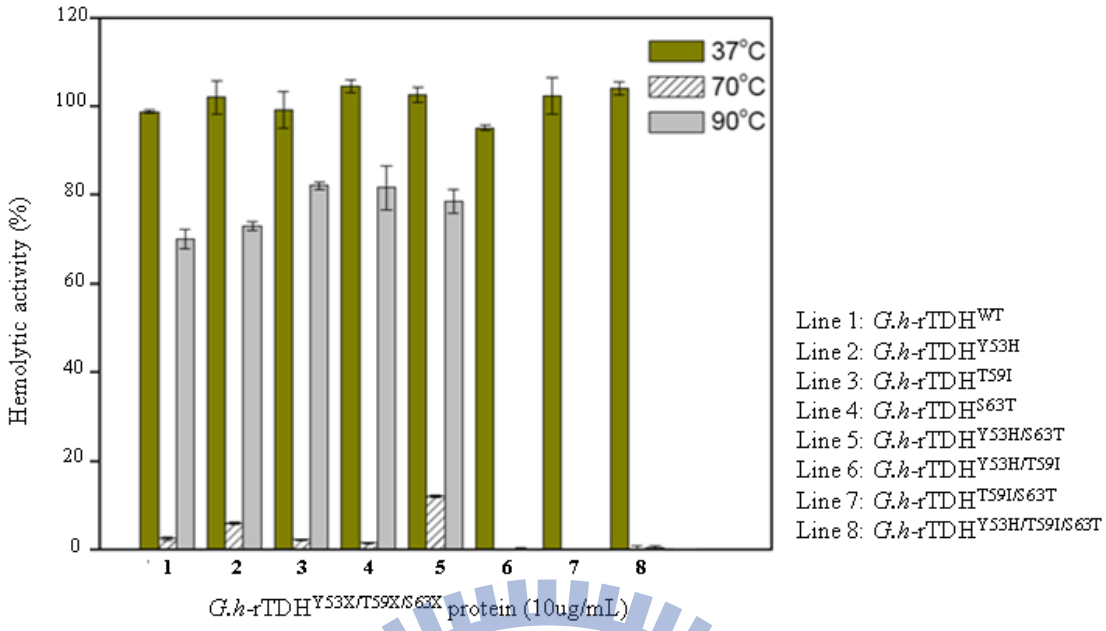

FIGURE 11. The hemolytic activity of various *G.h*-rTDH$^{Y53A/T59B/S63C}$ mutants after different temperature pre-treatments, coupled with a rapid cooling treatment. Data are presented as the means for triplicate experiments. Error bars represent standard deviations (SD).

4.8 Analysis of *G.h*-rTDH$^{Y53A/T59B/S63C}$ thermostability by difference scanning calorimetry

DSC measurements involve the heating of a sealed sample of protein solution at a constant rate of temperature increase. As long as no other process occurs in the solution that releases or takes up heat, the temperature of the solution will rise monotonically with the instrumental heating (electrical power input). The DSC profile provides much valuable information, including the temperature at which the maximum excess heat capacity occurs, called "T_{max}"; the area under the curve, obtained by integration using the software supplied with the instrument, gives "the enthalpy of denaturation"; the width of the peak at half of the maximum excess heat capacity is "full width at half maximum" (FWHM), which is an indication of the

co-operativity of the protein structure[36]. The calorimetric scan of TDH^{WT} and other TDH mutations in 10 mM Kpi (pH 7.0) were characterized by a single peak. The transition temperature of those proteins from low to high were 51.8^{o}C (*G.h*-rTDH^{T59I}), 52^{o}C (*G.h*-rTDH^{Y53H}), 55.3^{o}C (*G.h*-rTDH^{S63T}), 56.3^{o}C (*G.h*-rTDH$^{Y53H/S63T}$), 56.6^{o}C (*G.h*-rTDH^{WT}), 57.1^{o}C (*G.h*-rTDH$^{T59I/S63T}$), 58^{o}C (*G.h*-rTDH$^{Y53H/T59I}$), 58.4^{o}C (*G.h*-rTDH$^{Y53H/T59I/S63T}$), respectively. Those proteins without Arrhenius effect including *G.h*-rTDH$^{Y53H/T59I/S63T}$, *G.h*-rTDH$^{Y53H/T59I}$ and *G.h*-rTDH$^{T59I/S63T}$ have the top three T_m values, and obtained a wider FWHM, indicating that during the unfolding process by increasing temperature the more entropy is needed to disrupt the intramolecular interaction with those proteins, and more stable and compacted structures than others were conserved in these mutants. The *G.h*-rTDH^{T59I} and *G.h*-rTDH^{Y53H} have the lowest T_m values, indicating that these proteins were more unstable than others during the heat-induced denaturation.

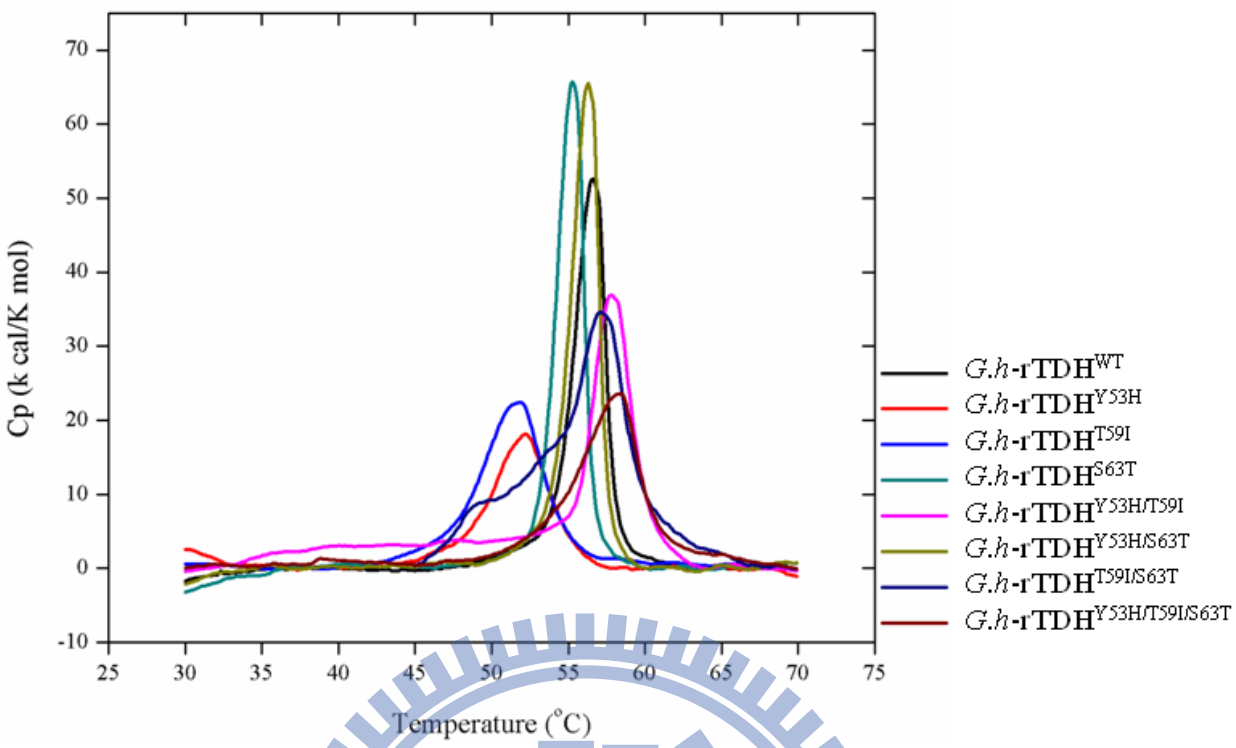

FIGURE 12. The DSC result. Corrected DSC thermograms of *G.h*-rTDH$^{Y53A/T59B/S63C}$ in 10 mM Kpi buffer at pH 7.0.

4.9 Analyze the secondary structure change of various *G.h*-rTDH$^{Y53A/T59B/S63C}$ mutants by circular dichroism spectroscopy

The change of secondary/tertiary structure caused by the thermal denaturation of *G.h*-rTDH in Kpi buffer (pH 7.0) was examined by circular dichroism (CD) spectra. At temperatures below 50℃, all proteins exist in a native state characterized by a β-rich secondary structure with a pronounced minimum at 218 nm (Figure 13 (E)). Between 50-60^{o}C, proteins underwent an intermediate state as shown in (Figure 14 (E)). Interestingly, the melting temperature-curve (the T_m value was determined by previous DSC instrument) of CD spectra of *G.h*-rTDH$^{Y53H/T59I/S63T}$ was compared to that of *G.h*-rTDH^{WT} (Figure 14 (A)). However, *G.h*-rTDH$^{Y53H/T59I/S63T}$ protein does not transit from a β-rich structure into a α-rich structure until 75^{o}C, whereas *G.h*-rTDH^{WT} dramatically changes its conformation above 56.6^{o}C, indicating that

G.h-rTDH$^{Y53H/T59I/S63T}$ has a higher activation energy than that of *G.h*-rTDH^{WT} in their phase transition processes. The increase of temperature from 60-95^{o}C, the α-helix-rich structure content of *G.h*-rTDH$^{Y53H/T59I/S63T}$ was still retained, whereas that of *G.h*-rTDH^{WT} was decreased vividly. Interestingly, all *G.h*-rTDH proteins were not completely denatured even at 95^{o}C. In 10 mM Kpi buffer (pH 7.0), the temperature-induced conformational change of *G.h*-rTDH$^{Y53H/T59I/S63T}$ occurs in a two-state manner, while that of *G.h*-rTDH^{WT} is in a three-state manner. For other *G.h*-rTDH$^{Y53A/T59B/S63C}$ mutants, the similar spectrum changes, as that of *G.h*-rTDH$^{Y53H/T59I/S63T}$, (in either the far-UV CD spectra or DSC data) were observed in *G.h*-rTDH$^{T59I/S63T}$ and *G.h*-rTDH$^{Y53H/T59I}$ mutants, from which both of them lost its Arrhenius effect after continuing heating, followed by a rapid cooling treatment (Figure 13 (B)). However, all proteins that have an Arrhenius effect, except for *G.h*-rTDH^{Y53H} *G.h*-rTDH^{T59I} and *G.h*-rTDH^{S63T} mutants, must undergo a transition state prior to the formation of an unfolded state after a thermal denaturation treatment. In the far-UV CD spectra, the complete collapse of its secondary structure was characterized in the *G.h*-rTDH^{Y53H} *G.h*-rTDH^{T59I} and *G.h*-rTDH^{S63T} mutants at temperatures above 56^{o}C and 60^{o}C, respectively (Figure 13 (C)). The *G.h*-rTDH$^{Y53H/S63T}$ CD spectrum is observed to occur between *G.h*-rTDH^{WT} and *G.h*-rTDH$^{Y53H/T59I/S63T}$ (Figure 13 (D)).

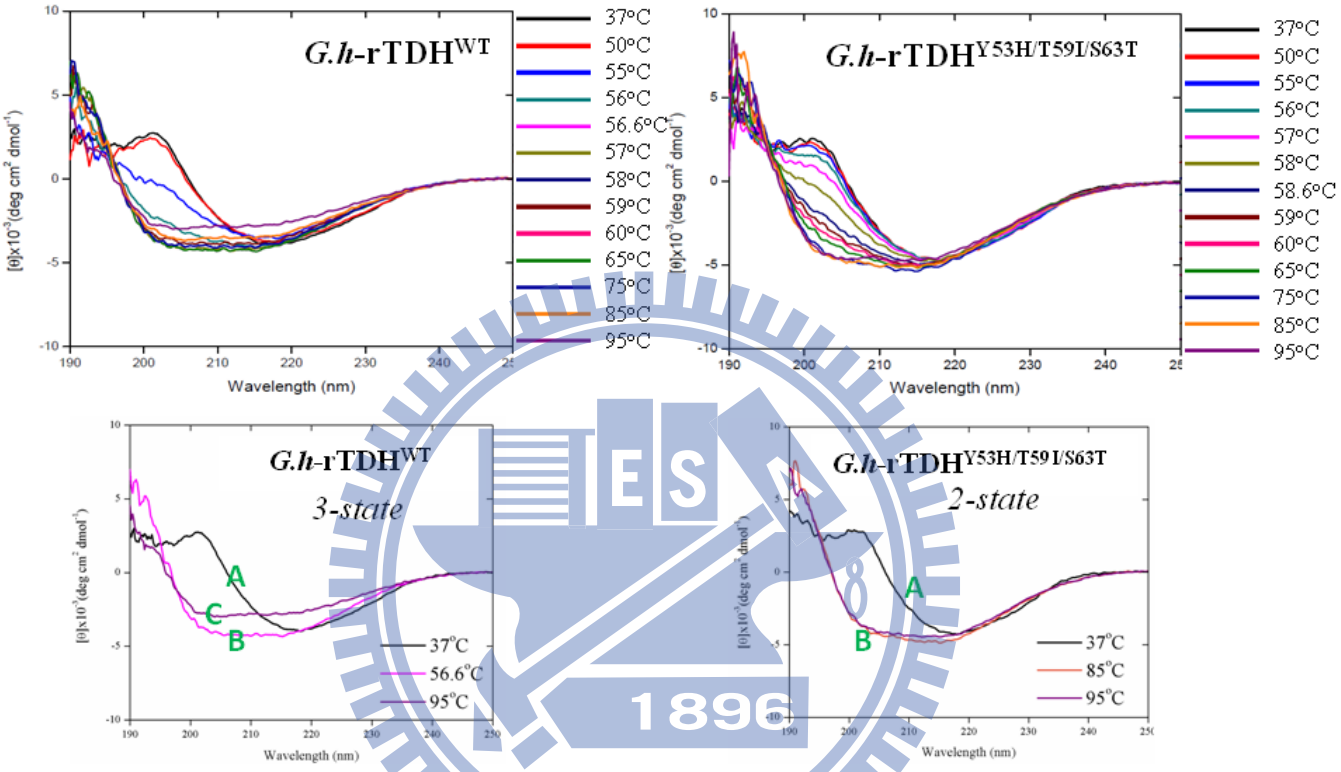

FIGURE 13. (A)The CD spectrum of *G.h*-rTDH^{WT} and *G.h*-rTDH$^{Y53H/T59I/S63T}$ and the *G.h*-rTDH^{WT} show three-state and *G.h*-rTDH$^{Y53H/T59I/S63T}$ show two-state manner when heat the temperature.

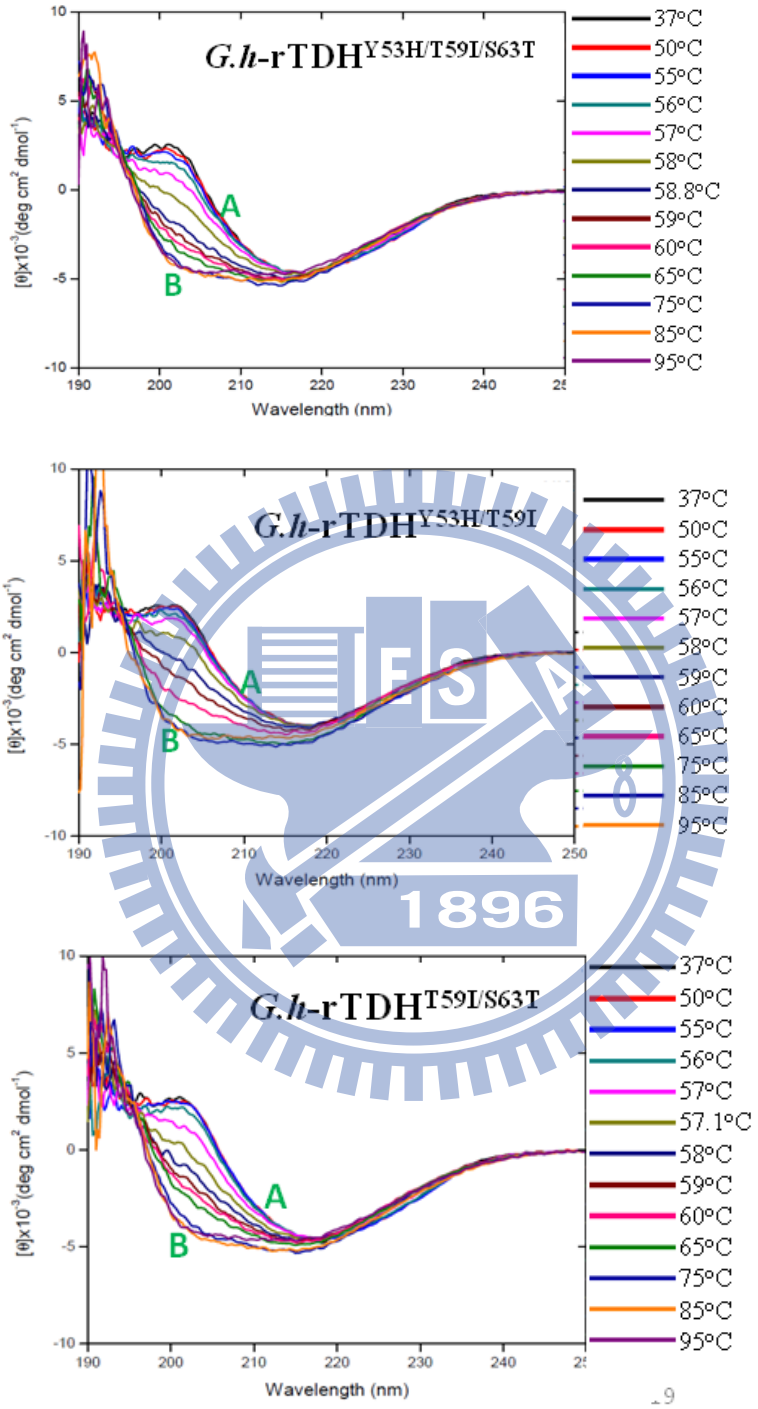

FIGURE 13. (B) The CD spectrum of *G.h*-rTDH$^{Y53H/T59I/S63T}$, *G.h*-rTDH$^{Y53H/T59I}$ and *G.h*-rTDH$^{T59I/S63T}$ which are deficiency the Arrhenius effect.

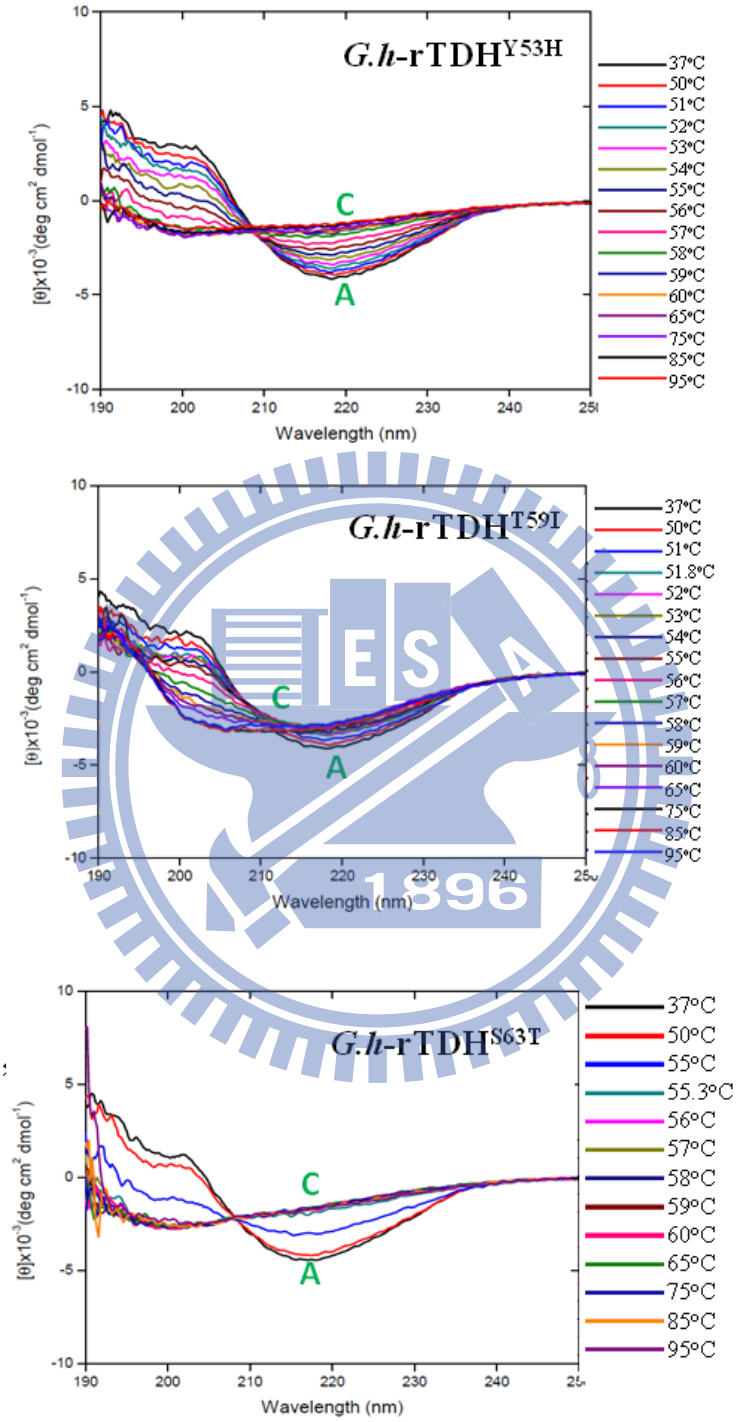

FIGURE 13. (C) The CD spectrum of *G.h*-rTDH^{Y53H}, *G.h*-rTDH^{T59I} and *G.h*-rTDH^{S63T} which are process the Arrhenius effect.

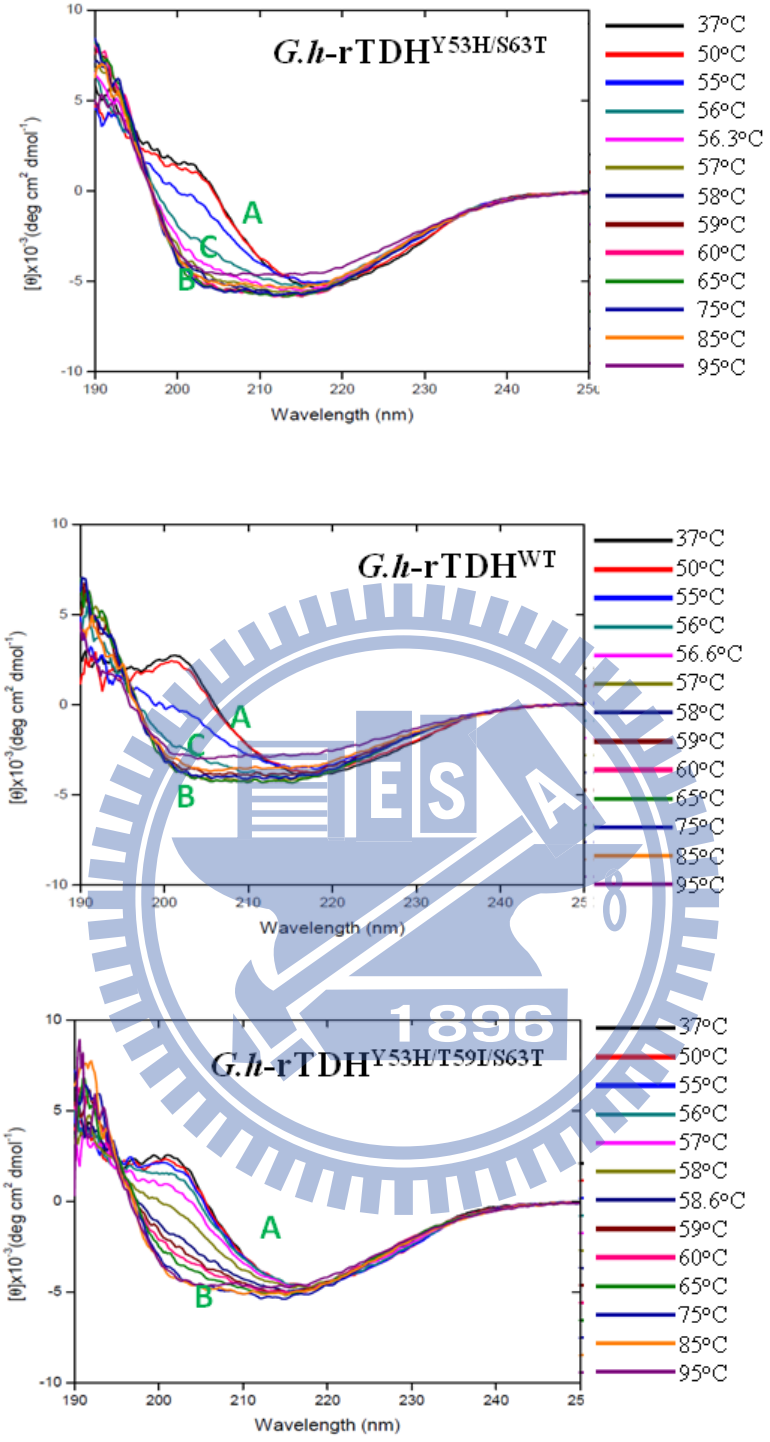

FIGURE 13. (D) The CD spectrum of *G.h*-rTDH^{WT}, *G.h*-rTDH$^{Y53H/T59I/S63T}$, and *G.h*-rTDH$^{Y53H/S63T}$. The *G.h*-rTDH$^{Y53H/S63T}$ pattern is between *G.h*-rTDH^{WT} and *G.h*-rTDH$^{Y53H/T59I/S63T}$.

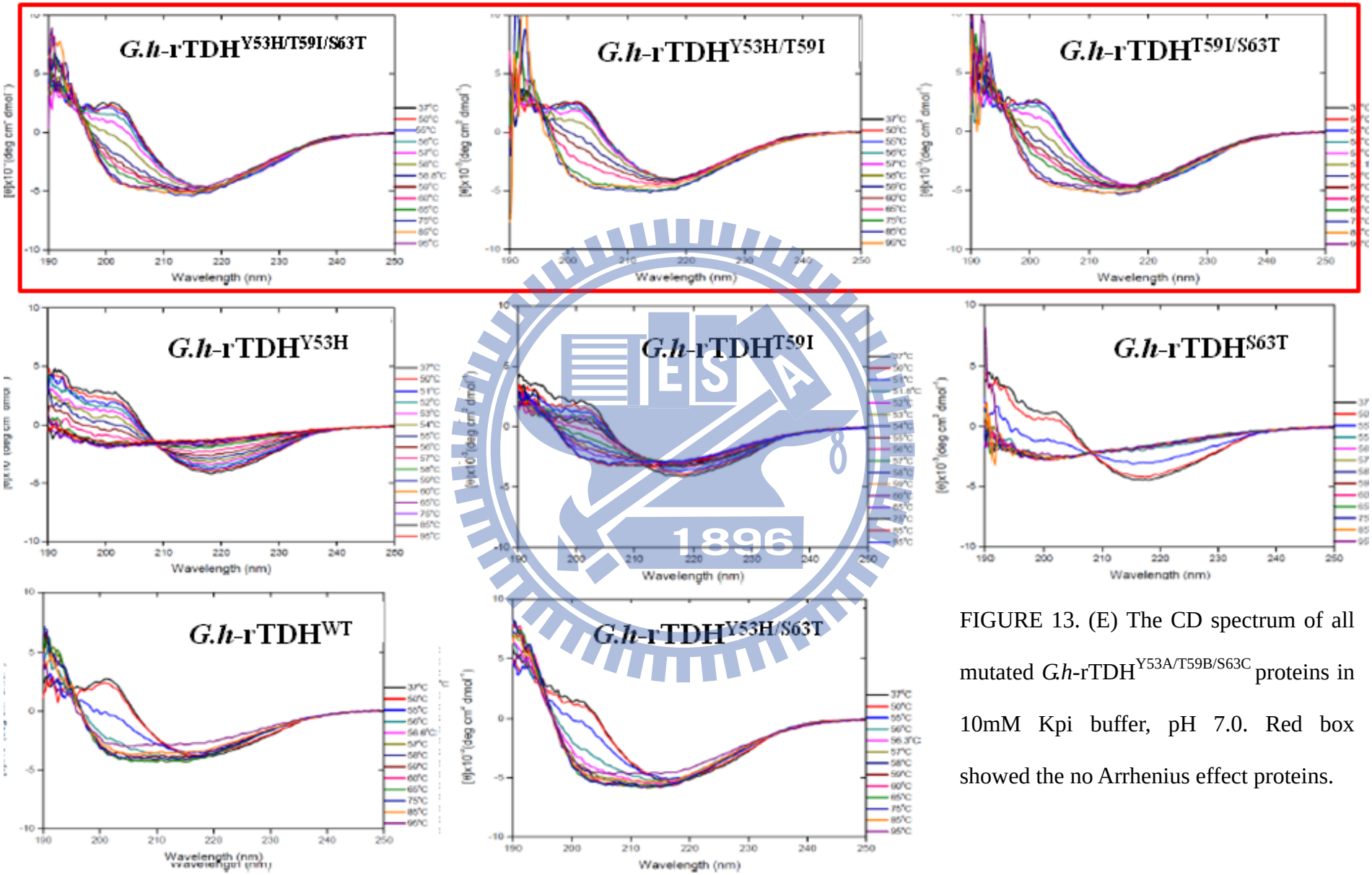

FIGURE 13. (E) The CD spectrum of all mutated *G.h*-rTDH$^{Y53A/T59B/S63C}$ proteins in 10mM Kpi buffer, pH 7.0. Red box showed the no Arrhenius effect proteins.

4.10 Morphology examination and MTT assay for *G.h*-rTDH$^{Y53A/T59B/S63C}$ of the cytotoxicity and cytoviability effect on AGS cells

To investigate the cytotoxicity of purified *G.h*-rTDH$^{Y53A/T59B/S63C}$ proteins on mammalian cells, the human stomach epithelial cell line, AGS, served as an *in vitro* model. The morphological change of AGS cells could be visually assessed in the absence or presence of *G.h*-rTDH$^{Y53A/T59B/S63C}$ exposure for 30 min with 10 μg/mL *G.h*-rTDH$^{Y53A/T59B/S63C}$ at 26^{o}C. Among the result of these mutants, the morphology of AGS cells were changed, including the membrane blebbing, the cell detachment, loss of cell cytoplasm with cell shrinkage, and the reduction of nuclei size. *G.h*-rTDH$^{Y53A/T59B/S63C}$ mutants have different levels of cytotoxicity on the AGS cell line and the cell morphology has different degrees of damage during the treated duration, as shown in Figure 14. When AGS cells were exposed to the *G.h*-rTDH$^{Y53H/S63T}$ mutant, cell morphology has a dramatic change. When AGS was exposed to other mutants like *G.h*-rTDH$^{Y53A/T59B/S63C}$ except for *G.h*-rTDH$^{Y53H/T59I/S63T}$ and *G.h*-rTDH$^{T59I/S63T}$, the cell morphology had obvious changes within the initial 5 min, and the complete dramatic change in the morphology was observed in 30 min. In addition, we used the MTT assay (Figure 16) to analyze the cytoviability when cell was treated with different concentrations of *G.h*-rTDH$^{Y53A/T59B/S63C}$ (100 μg/mL and different serial dilutions in ten-fold increments) in 1 h at 37^{o}C. Accordingly, the inhibitory concentration (IC_{50}) value of *G.h*-rTDH$^{Y53H/T59I}$ (defined as the drug concentration at which cell growth was inhibited by 50%) at 10 μg/mL was the lowest observed, and the IC_{50} value of *G.h*-TDH$^{Y53H/S63T}$ inhibitory concentration (IC_{50}) at 2 μg/mL was the highest assessed from the dose-response curves shown in Figure14.

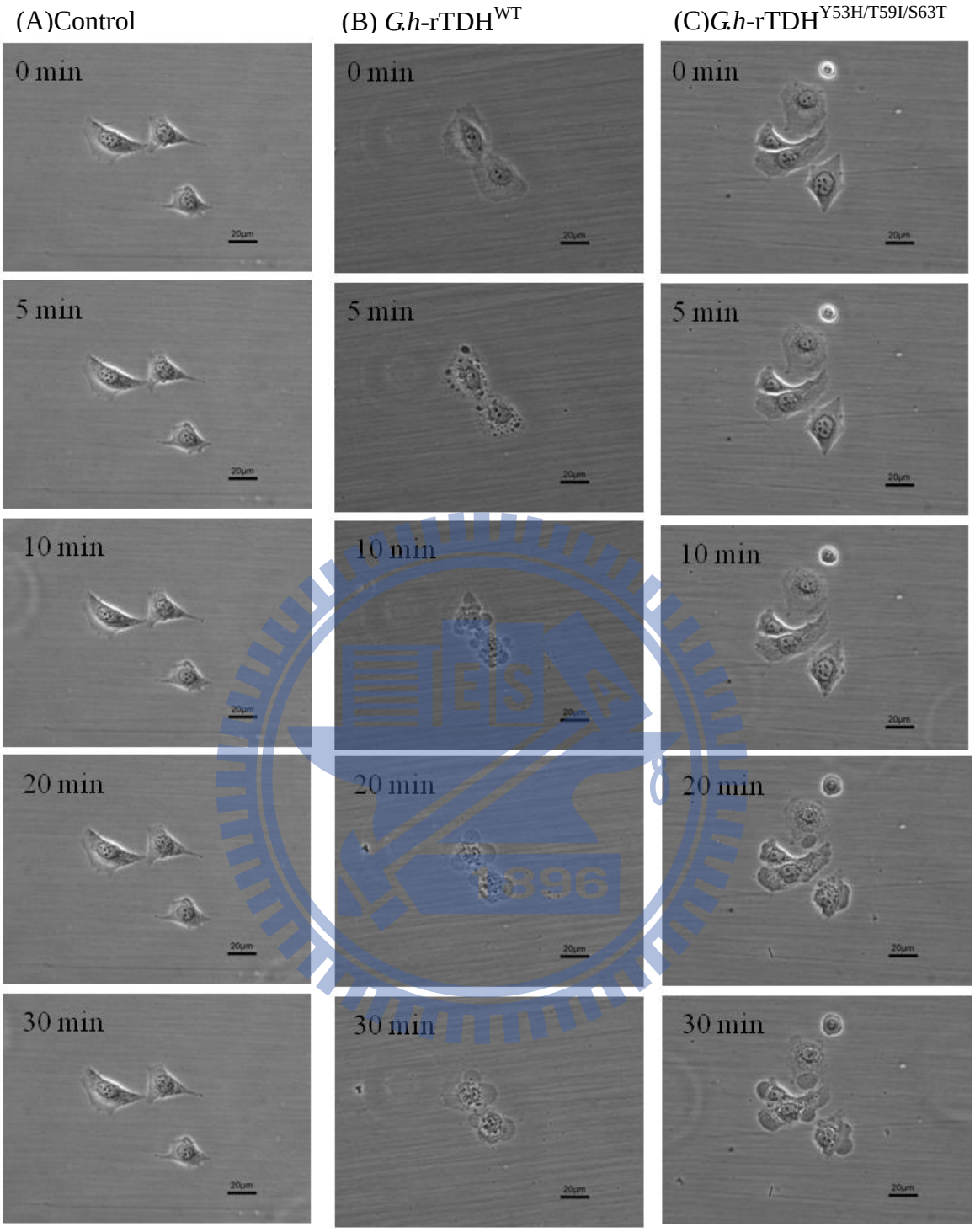
(A)Control
(B) G.h-rTDH^WT
(C)G.h-rTDH^Y53H/T59I/S63T
0 min
5 min
10 min
20 min
30 min
20μm

(D) *G.h*-rTDH^{Y53H} (E) *G.h*-rTDH^{T59I} (F)*G.h*-rTDH^{S63T}

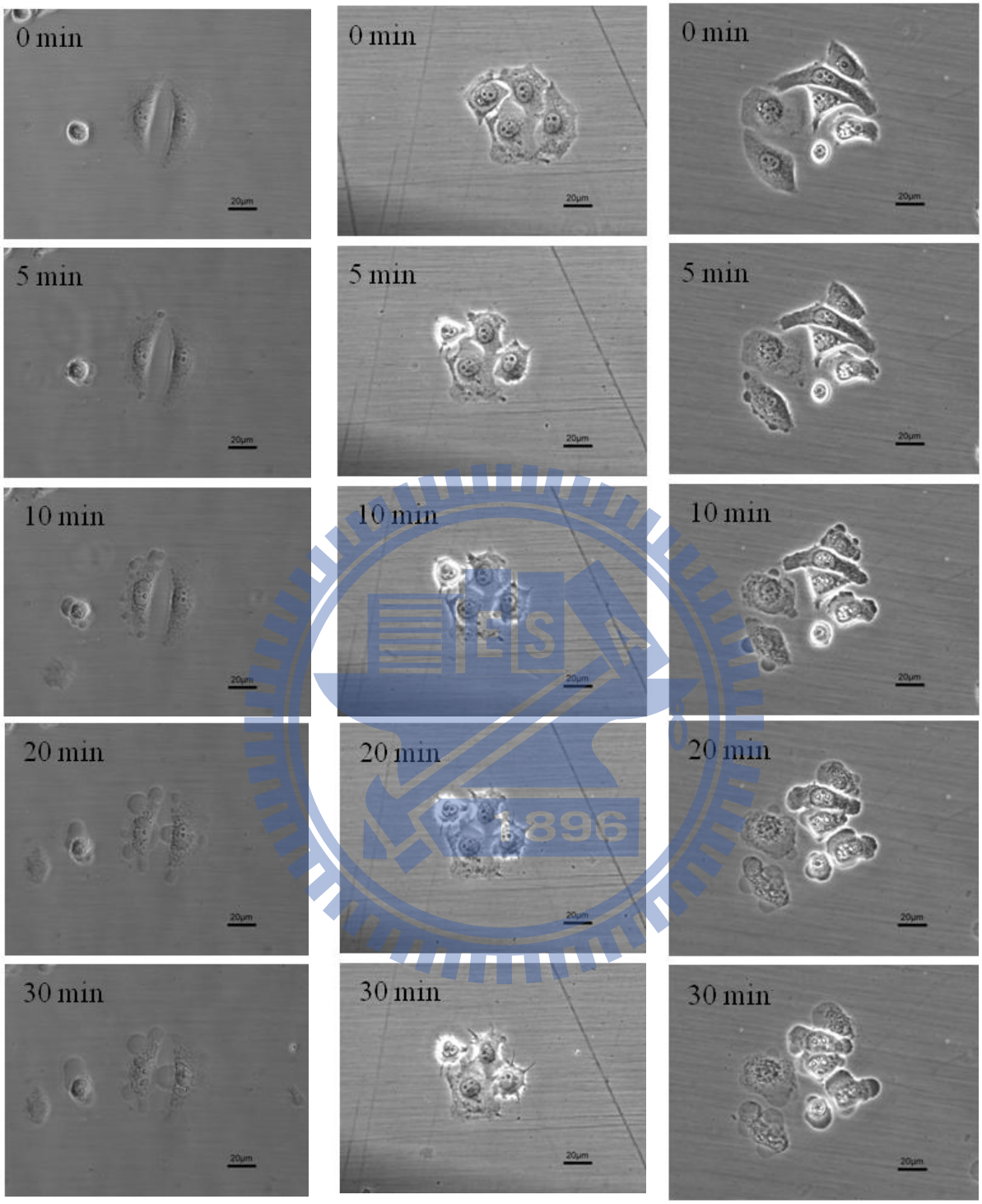

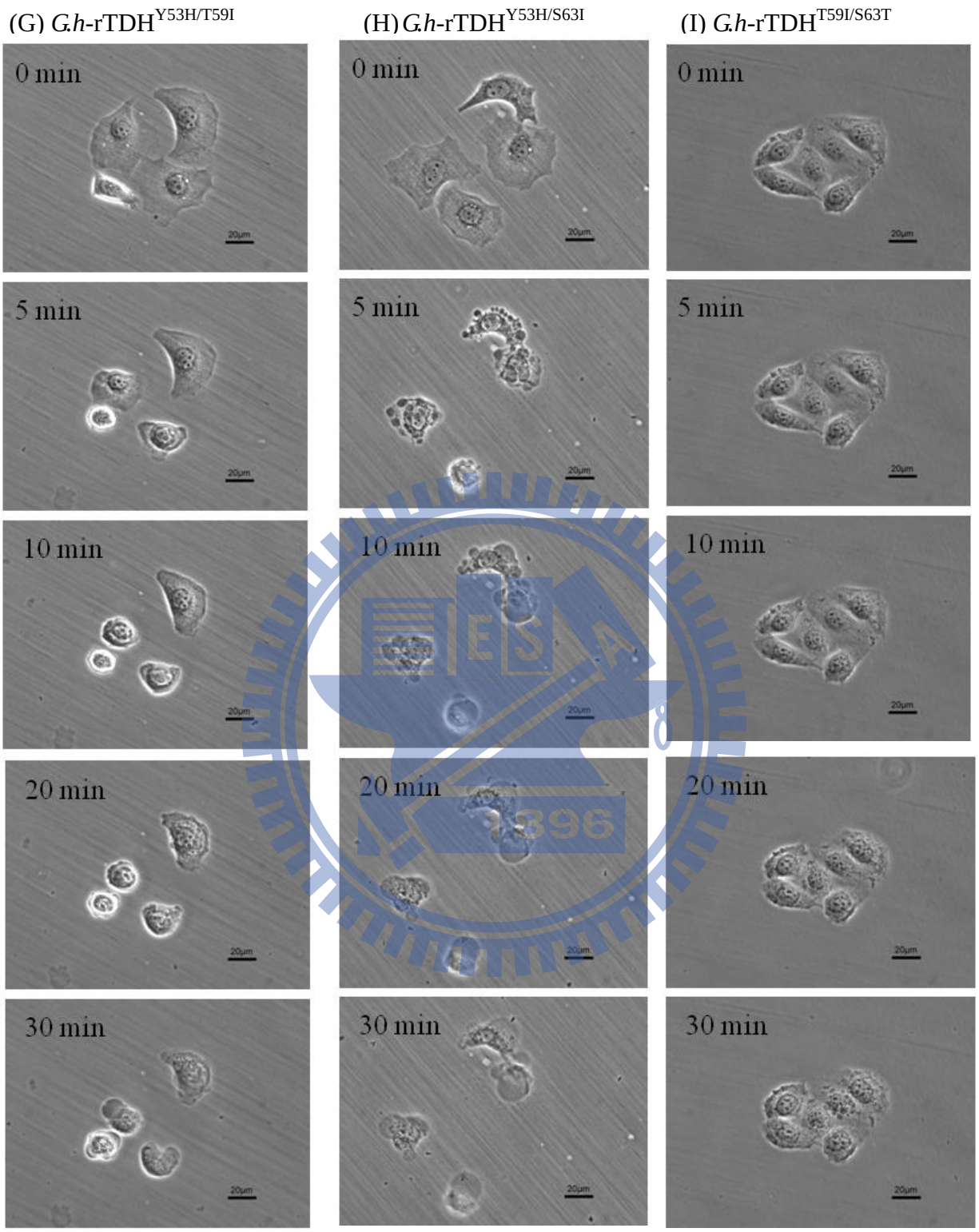

FIGURE 14. Cell morphology. AGS cell line was exposed *G.h*-rTDH$^{Y53A/T59B/S63C}$ 10ug/mL in 30min at 26^{o}C.

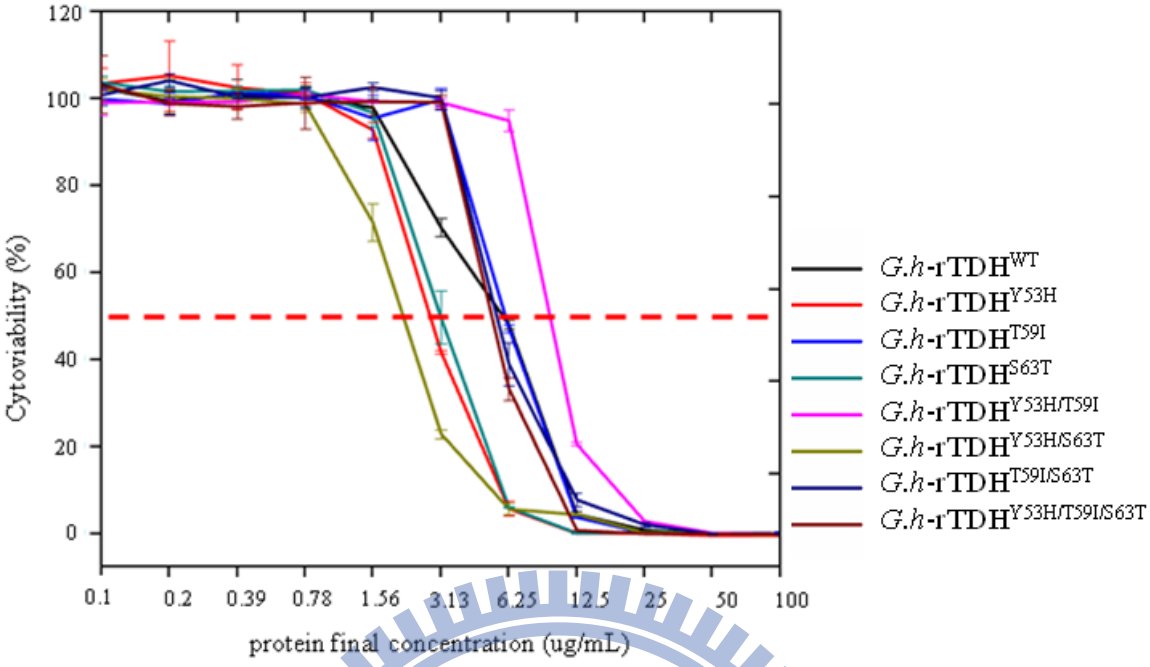

FIGURE 15. MTT assay results of various *G.h*-rTDH$^{Y53A/T59B/S63C}$ mutants. The cytoviability decreased in proportion to different concentrations of *G.h*-rTDH (100 μg/mL and ten-folded serial dilutions) in 1 h at 37°C. Data are presented as the means for triplicate experiments. Error bars represent the standard deviations (SD)

4.11 Thioflavin T florescence assay

Thioflavin T fluorescence assay was used to determine the fibrils contents of various TDH mutants, which are generated from a thermal-pretreatment of TDH mutants at either 37 °C, 70 °C, or 90 °C coupled with a rapid cooling, respectively. According to the result of ThT assay, the filber contents of *G.h*-rTDH^{T59I}, *G.h*-rTDH^{S63T}, *G.h*-rTDH$^{Y53H/T59I}$, *G.h*-rTDH$^{Y53H/S63T}$, *G.h*-rTDH$^{T59I/S63T}$, and *G.h*-rTDH$^{Y53H/T59I/S63T}$ generated from a 90°C thermal pre-treatment coupled with rapid cooling are higher than that of TDH mutations generated from a 70°C thermal pre-treatment coupled with rapid cooling. Comparably, the fibrils contents of *G.h*-rTDH^{WT} and *G.h*-rTDH^{Y53H} are

similar at either fiber generation from a 90°C thermal pre-treatment or a 70°C thermal pre-treatment, coupled with a rapid cooling, respectively.

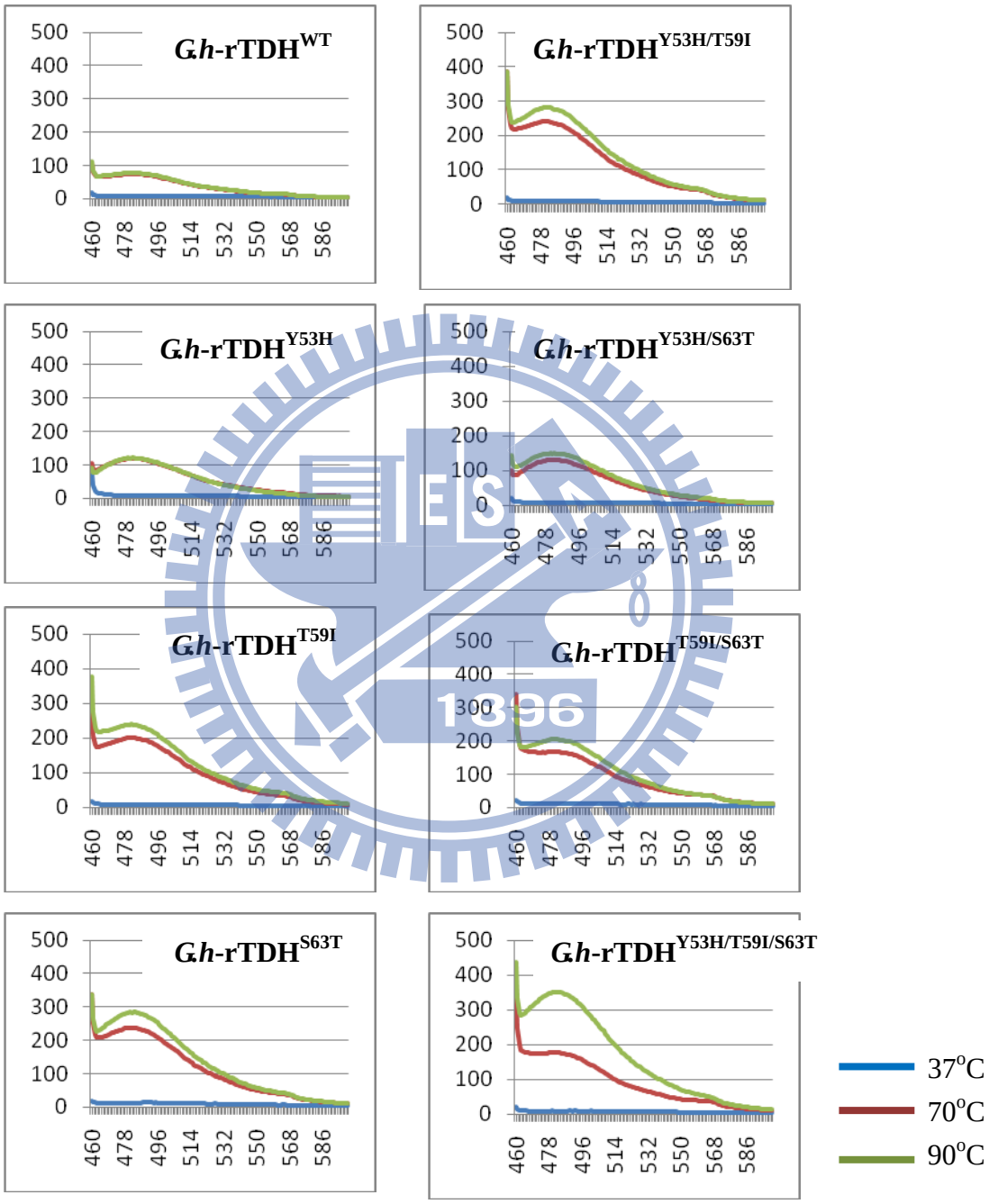

FIGURE 16. Thioflavin T florescence assay result. Those curves are presented as the means for triplicate experiments.

Chapter 5

Discussion

The data in this thesis showed that the thermostable direct hemolysin (TDH) of *G. hollisae* from BCRC 15890 strain exhibited a distinct biophysical characterization from that of the historically published *tdh* gene in NCBI data bank, *G. hollisae* 9041. First, three distinct amino acid changes, *i.e.* Tyr53→His53, Thr59→Ile59, and Ser63→Thr63 were observed from the pairwise sequence alignment of these two same sources TDH. Subsequently, seven *G.h*-rTDH mutants comprising the combination of these three diverse amino acids, *i.e.* *G.h*-rTDH^{Y53H}, *G.h*-rTDH^{T59I}, *G.h*-rTDH^{S63T}, *G.h*-rTDH$^{Y53H/T59I}$, *G.h*-rTDH$^{Y53H/S63T}$, *G.h*-rTDH$^{T59I/S63T}$, and *G.h*-rTDH$^{Y53H/T59I/S63T}$ mutants were thus constructed and used to have various biophysical characterizations. Among these mutations, *G.h*-rTDH$^{Y53/T59I}$, *G.h*-rTDH$^{T59I/S63T}$, and *G.h*-rTDH$^{Y53H/T59I/S63T}$ lost its function of hemolytic activity on erythrocyte cells via first heating at 90^{o}C for 30 min, coupled with a rapid cooling. The phenomenon of heating inactivation but functional reactivation via further cooling treatment was represented as “Arrhenius effect”, and it is one of significant feature of wild type TDH from *G. hollisae.* Interestingly, at least mutagenic two amino acid position, *i.e* *G.h*-rTDH$^{Y53H/T59I}$, *G.h*-rTDH$^{T59I/S63T}$ and *G.h*-rTDH$^{Y53H/T59I/S63T}$mutants, dramatically influenced their Arrhenius effect, except for *G.h*-rTDH$^{Y53H/S63T}$ mutant where a slight enhancement of hemolytic activity on erythrocyte cells was observed.

Moreover, the DSC experimental illustration these *G.h*-rTDH mutants are in good agreement with the corresponding result from the CD–melting curves of these mutants which were measured by monitoring the temperature change. From DSC data,

the *G.h*-rTDH$^{Y53H/T59I/S63T}$ protein showed a stable conformation than that of *G.h*-rTDH^{WT} protein. Interestingly, no Arrhenius effect proteins involving *G.h*-rTDH$^{Y53H/T59I}$, *G.h*-rTDH$^{T59I/S63T}$, and *G.h*-rTDH$^{Y53H/T59I/S63T}$ mutants undergo two-state conformational transition change from β-rich structure into a α-rich structure, from the recorded CD spectra during the increasing temperature. Moreover, even at 95^{o}C those mutant proteins retain the compact secondary structure elements without any complete unfolding, suggesting that the fiber form state existed and caused the proteins to have Arrhenius effect deficiency. The rapid cooling treatment still remains the protein conformation at its fiber form that is a non-toxin form. In contrast, for the single mutation proteins possessing Arrhenius effect, *i.e.* *G.h*-rTDH^{Y53H} *G.h*-rTDH^{T59I} and *G.h*-rTDH^{S63T}, the secondary structure collapsed also in a two-state manner. In the *G.h*-rTDH^{Y53H} and *G.h*-rTDH^{S63T}, when heat temperature above 60^{o}C their secondary structure complete collapse and protein from β-rich structure into unfold state not through α-rich structure. And the *G.h*-rTDH^{Y53H} has more compact than *G.h*-rTDH^{S63T} show in figure 16. Interestingly, *G.h*-rTDH^{T59I} remained partial α-rich structure when heat to high temperature. Those single mutation proteins when they through the transition state were more unstable than others. Under the heating temperature, the G.h-rTDH$^{Y53H/S63T}$ protein exhibited a unique characteristic of secondary structure between the data of no-Arrhenius effect proteins and Arrhenius effect proteins. For Arrhenius effect proteins, the intensity of the minima at 218 nm, which represents a β-rich structure, occurs at the low measured temperature that protein exist a native form, decreases the content between 50^{o}C to 60^{o}C and completely disappears above at 60^{o}C and convert to a α-rich structure or a unfolded state. We think those proteins possessing Arrhenius effect at the high temperature might become an unfolded structure state via heating, and it could return to form functional form for keeping its hemolytic activity after rapid cooling.

However, there is no difference among the observations of the experimental results in the melting curve of CD spectra, SDS-PAGE, and native-PAGE either in stacking or separating gel with all proteins treated with rapid or slow cooling after a first heating. In the previous study, the crude protein involving TDH from *V. parahaemolyticus* has similar phenomenon in SDS-PAGE where no band is visualized at 22 KDa. They think there is an inactivating factor to inhibit the TDH hemolysis function and the factor processes proteolytic activity that can digest TDH[30]. In the other hand, Takashi, F. et. al, suggested that the *V. parahaemolyticus* TDH process Arrhenius effect phenomena because of the protein structure can recover to its native form and remain the hemolysis function when heated high temperature coupled by a rapid treatment[24]. However, in our results, those *G.h*-rTDH$^{Y53A/T59B/S63C}$ remained the secondary structure formation of high temperature when after treatment a rapid cooling or a slower cooling. In this part, the exact reason of the thermal-induced hemolytic activity change as well as its conformational change of *G.h*-rTDH$^{Y53A/T59B/S63C}$ protein is still unknown. We think the different cooling rate and protein structure stability might influence the protein refolding pathway, thus causing the distinct result. Additionally, the lacking of the detailed structural information in a CD spectrum might also result in the difficulty for interpretation of real-time actual structural features of proteins such as α/β barrels.

On the other hand, the experimental results demonstrated that various *G.h*-rTDH$^{Y53A/T59B/S63C}$ mutants influenced the in cytotoxicity activities against AGS cell lines, and hemolytic activity against erythrocytes. However, even the cytotocixity and hemolytic activity are different but similar tendency existed. Matsuda *et. al* have reported that the lipid rafts including sphingomyelin is essential for cytotoxicity of TDH from *V. parahemolytics*, but not associated with hemolytic activity[37]. In my

study, the cytotoxicity induced by *G.h*-rTDH$^{Y53A/T59B/S63C}$ mutants caused different level cell damage, which might associated with the interaction of *G.h*-rTDH$^{Y53A/T59B/S63C}$ and lipid rafts from AGS membrane. The slight and critical cytotoxicity induced by *G.h*-rTDH$^{Y53H/T59I}$ and *G.h*-rTDH$^{Y53H/S63T}$, respectively, further confirm this theory that it's important for the association of TDH with lipid rafts. The high interaction between the lipid rafts and *G.h*-rTDH$^{Y53H/S63T}$ mutants for its target molecules on the plasma membrane of eukaryotic cells cause the critical damage to AGS cell. In 1997, Guangqing T., et. al. reported the mutant cell line, MR-T1, was over 200 times more resistant to the cytotoxic activity of TDH from *V. parahaemolyticus* than Rat-1, the most sensitive cell line[25]. Additionally, different cell lines has varying susceptibility to TDH[25]. Those evidences suggested that the cell membrane contents affected cytotoxicity of TDH. Moreover, the hemolytic activity induced by *G.h*-rTDH$^{Y53A/T59B/S63C}$ mutants for caused the differential level damage on human erythrocytes. Previous reports has revealed that a mutanted toxin of TDH from *V. parahemolytics*, R7, which has a single amino acid substitution of serine for glycine 62, a deficiency in hemolytic activity[33]. The corresponding mutant in *G. hollisae*, *G.h*-rTDH^{G62A} also displayed a dramatic decreased hemolytic activity in our previous study, indicating that the glycine 62 is a important position for the hemolytic activity. Interestingly, the different hemolytic activity was observed when *G.h*-rTDH^{WT} treat with various mammal erythrocytes. In the previous study, Tang G. et. al. use monoclonal antibodies to detect the functional domain of TDH from *V. parahaemolyticus*[38]. TDH bound to the erythrocytes with its *N*-terminal region and caused the pore formation by using its *C*-terminal region[38]. However, the mechanism of TDH's hemolysis activity or its target molecules on the plasma membrane of erythrocytes cells still remains unclear. In this study, the protein of various *G.h*-rTDH$^{Y53A/T59B/S63C}$ mutants are near the glycine 62 position. The single mutantion,

except for *G.h*-rTDH^{Y53H}, examined the hemolysis activity higher than that of *G.h*-rTDH^{WT}, whereas the double mutation, except for *G.h*-rTDH$^{Y53H/S63T}$, decreased their hemolytic activity. Moreover, the *G.h*-rTDH$^{Y53H/S63T}$ mutant has dominate sensitivity in the cytotoxicity and hemolytic activity among at all *G.h*-rTDH$^{Y53A/T59B/S63C}$ mutants. Nevertheless, the structure aligment of *G.h*-rTDH^{WT} and *G.h*-rTDH$^{Y53H/T59I/S63T}$ showed a high similarity, even a different biophysical and physiology characterization existed between two TDH proteins. These findings confirm that the protein monomer structure is not the key point that dramatically affects the hemolytic activity. Yanagihara et.al. have reported that the TDH from *V. parahemolytics* form a tetramer with a central pore and it's indispensable for hemolytic activity[39]. In the staphylococcal alpha-hemolysin and equinatoxin II from the sea anemone are also pore-form toxin, when caused the erythrocytes damage the soluble monomer into the extra-bacterial space, and target to the host cell membrance when it oligomerized to form a pore[40,41]. The mutanted position of Tyr53, Thr59, and Ser63 of *G.h*-rTDH^{WT} are exposed outside of protein surface, which might affect the ability to form the tetramer conformation and to influence the binding ability of TDH to the erythrocytes cells membrane or hemolysis. However, the precise structure of the intramolecule interaction and the mechanism of these *G.h*-rTDH$^{Y53A/T59B/S63C}$ mutants are still unknown. Furthermore, the mechanism of action of pore-forming *G.h*-rTDH^{WT} toxin is not clear. Pore-forming toxin affect the permeability of target cells including erythrocyte and nucleated cell by forming pores on their plasma membrane even the target organisms might overcome these effects by triggering intracellular responses that have evolved as defense mechanisms to the *G.h*-rTDH^{WT}.

Chapter 6

Conclusions and Future Perspectives

Thermostable direct hemolysin (TDH) is composed of 165 amino acids and is considered a pore-forming toxin, which may be important in both pathogenesis and virulence. Moreover, the *tdh* gene or the produced TDH protein was observed in various vibrio strains including *V. cholera* non-O1, *V. parahaemolyticus*, *V. mimicus* and *V. alginolyticus*, where the biophysical and physiological characterizations of those TDH are still unknown except for that from *V. parahaemolyticus*. During the cytotoxicity experiment, we discovered additional questions and phenomena, for example, how does TDH enter the erythrocyte and nucleated cell, and does TDH interact with DNA? Based on the previous results in our lab, the *G.h*-rTDH^{WT} treated in different sources of erythrocyte produces different levels of damage. We think possibly the phenomenon is connecting with the content of cell membrane via lipid rafts. *G.h*-rTDH^{WT} and *G.h*-rTDH^{G62A} produced two proteins where the hemolytic activity and the cytotoxicity at 37^{o}C was entirely different. *G.h*-rTDH^{WT} was absolutely effective, and *G.h*-rTDH^{G62A} was not. We can use two proteins to confirm the mechanism of TDH entry to the erythrocyte and nucleated cell. On the other hand, in the florescence image data, we discovered that the *G.h*-rTDH^{WT} conjugate FITC was largely located on the cell nucleus about 20 minutes later. Does the *G.h*-rTDH^{WT} interact with DNA? Fourier transform infrared (FTIR) difference spectroscopy may provide the powerful information to study the protein-DNA interaction signal. The hemolytic activity of most hemolysins can inhibit or enhance its efficiency by addition of metal ions, the *G.h*-rTDH^{WT} may possess similar capabilities.

6.1 *G.h*-rTDH^{WT} enters the erythrocyte and nucleated cell

In the *vibrio parahaemolyticus* the hemolytic activity and the cytotoxicity are different pathways. For the cytotoxicity, the level of damage connects with the lipid raft and via protein interactions. But the hemolytic activity does not show a relationship with the lipid raft. The lipid raft involved liposomes, which can influence the receptor associations of the *G.h*-rTDH^{WT} and the level of cell damage.We want to elucidate the pathway that *G.h*-rTDH^{WT} utilizes to attack the cell.

6.2 *G.h*-rTDH^{WT} interaction with DNA

Fluorescence Polarization is a method used in diverse areas in scientific research, including ligand binding, immunoassay and high-throughput screening. The method was described early in 1926 by Perrin. The methods were modulated by Walter Dandliker in 1960s to study antibody- antigen interaction, and were referred as to fluorescence polarization immunoassays (FPIA). However, the method was popular because it is very efficient to use and low-cost. It is based on the fluorescence intensity to detect the protein and target substance interaction, where the florescence was conjugated to DNA. We will use the fluorescein isothiocyanate (FITC) as florescence probe, the excitation and emission wavelengths are approximately 495 nm and 521 nm, respectively. The *G.h*-rTDH^{WT} mixes with DNA for a few minutes to produce the *G.h*-rTDH^{WT}-DNA complex, and the FP value is measured to compare the positive and negative control values. The polarization is a property of a fluorescent molecule. By using the principle of this characteristic, the rotation and vibration behavior of fluorescent molecule could be detected in solution. The *G.h*-rTDH^{WT}-DNA complex was larger than the DNA and protein, and the molecular rotation was slower and the polarization of light remained, where the FP value was higher than the DNA or protein.

6.3 *G.h*-rTDH^{WT} interaction with metal ions

The functional residues in protein generally interacted with the metal ion, which serves as a special ligand. The metal ion may affect the protein, including influence stability of the conformation, enhance or reduce the effect. Usually a metal ion will bind to a hydrophobic area. The metal ions potentially involved including Zn^{2+}, Ca^{2+}, Mg^{2+}, Mn^{2+} will be examined. Metal ion binding to the *G.h*-rTDH^{WT} may affect the biological activity including hemolytic activity and cytotoxicity. One assay that can be attempted would be to take a 10 μL volume of *G.h*-rTDH^{WT} (1 μg/mL) incubated with 10 μL of metal ions (20 mM) dissolved in 10 mM PBS (pH 7.0) at 37^{o}C for 1 h, then measure the hemolytic activity assay and the cytoviability assay.

Reference

(1) West, P. A. *Epidemiol Infect* **1989**, 103, 1-34.

(2) Tacket, C. O.; Brenner, F.; Blake, P. A. *J Infect Dis* **1984**, 149, 558-61.

(3) Baross, J.; Liston, *J. Nature* **1968**, 217, 1263-4.

(4) Wallace, R. B.; Battey, Y. M. *Med. J. Aust* **1971**, 1, 982.

(5) Dadisman, T. A.; Garber, H. *J. Am J Epidemiol* **1972**, 96, 414-26.

(6) Honda, T.; Iida., T. *Rev. Med. Microbiol.* **1993**, 106-13.

(7) Thompson, F. L.; Hoste, B.; Vandemeulebroecke, K.; Swings, *J. Int J Syst Evol Microbiol* **2003**, 53, 1615-7.

(8) Hickman, F. W.; Farmer, J. J., 3rd; Hollis, D. G.; Fanning, G. R.; Steigerwalt, A. G.; Weaver, R. E.; Brenner, D. J. J *Clin Microbiol* **1982**, 15, 395-401.

(9) Morris, J. G., Jr.; Miller, H. G.; Wilson, R.; Tacket, C. O.; Hollis, D. G.; Hickman, F. W.; Weaver, R. E.; Blake, P. A. *Lancet* **1982**, 1, 1294-7.

(10) Lowry P. W.; K, T. H. *J infect Dis*. **1986**, 154, 730-1.

(11) Abbott S. L. ; M., J. J. *Clin Infect Dis*. **1994**, 18, 310-2.

(12) Carnahan, A. M.; Harding, J.; Watsky, D.; Hansman, S. J *Clin Microbiol* **1994**, 32, 1805-6.

(13) Lesmana, M.; Subekti, D. S.; Tjaniadi, P.; Simanjuntak, C. H.; Punjabi, N. H.; Campbell, J. R.; Oyofo, B. A. *Diagn Microbiol Infect Dis* **2002**, 43, 91-7.

(14) Blake, P. A.; Weaver, R. E.; Hollis, D. G. *Annu Rev Microbiol* **1980**, 34, 341-67.

(15) Datta-Roy, K.; Baberjee, K.; De, S. P.; Ghose, A. C. *Appl Environ Microbiol* **1986**, 52, 875-9.

(16) Shirai, H.; Ito, H.; Hirayama, T.; Nakamoto, Y.; Nakabayashi, N.; Kumagai, K.; Takeda, Y.; Nishibuchi, M. *Infect Immun* **1990**, 58, 3568-73.

(17) Zhang, X. H.; Austin, B. *J Appl Microbiol* **2005**, 98, 1011-9.

(18) Honda, T.; Iida, T. *Rev. Med. Microbiol.* **1993**, 4, 106-13.

(19) Miyamoto, Y.; Kato, T.; Obara, Y.; Akiyama, S.; K., T.; Yamai, S. *J. Bacteriol* **1969**, 100, 1147-49.

(20) Sakazaki, R.; Iwanami, S.; Tamura, K. *Jpn J Med Sci Biol* **1968**, 21, 313-24.

(21) Goshima, K.; Owaribe, K.; Yamanaka, H.; Yoshino, S. *Infect Immun* **1978**, 22, 821-32.

(22) Sakurai, J.; Honda, T.; Jinguji, Y.; Arita, M.; Miwatani, T. *Infect Immun* **1976**, 13, 876-83.

(23) Tang, G. Q.; Iida, T.; Yamamoto, K.; Honda, T. *FEMS Microbiol Lett* **1995**, 134, 233-8.

(24) Fukui, T.; Shiraki, K.; Hamada, D.; Hara, K.; Miyata, T.; Fujiwara, S.; Mayanagi, K.; Yanagihara, K.; Iida, T.; Fukusaki, E.; Imanaka, T.; Honda, T.; Yanagihara, I.

Biochemistry **2005**, 44, 9825-32.
(25) Tang, G.; Iida, T.; Inoue, H.; Yutsudo, M.; Yamamoto, K.; Honda, T. *Biochim Biophys Acta* **1997**, 1360, 277-82.
(26) Nishibuchi, M.; Doke, S.; Toizumi, S.; Umeda, T.; Yoh, M.; Miwatani, T. Appl *Environ Microbiol* **1988**, 54, 2144-6.
(27) Hinestrosa, F.; Madeira, R. G.; Bourbeau, P. P. *J Clin Microbiol* **2007**, 45, 3462-3.
(28) Toshio, M.; Yoshifumi, T.; Jun, S.; Akiko, Y.; Sekiko, T. *Infect Immun* 1972, 6, 1031-1033.
(29) Michael, L. V.; L., P. V.; I., B. H. *Infect Immun* **1976**, 13, 1467-72.
(30) Yoshifumi, T.; Yayoi, h.; Sekiko, T.; Jun, S.; Toshio, M. *Infect Immun* **1975**, 12, 449-54.
(31) Yoshifumi, T.; Yayoi, h.; Toshio, M. *Infect Immun* **1974**, 10, 6-10.
(32) Hirotaka, H.; Toshio, K.; Tetsuya, I.; Takeshi, H. *Infect Immun* **2010**, 78, 1772-1780.
(33) Tetsuya, I.; Guang-Qing, T.; Sataporn, S.; Koichiro, Y.; Toshio, M.; Takeshi, H. *Toxicon* **1995**, 33, 209-16.
(34) Tung-Kung, W.; Yu-Kuo, W.; Yi-Chin, C. *J Bacteriol* **2007**, 189, 8215-23.
(35) Rosenfeld, J.; Capdevielle, J.; Guillemot, J. C.; Ferrara, P. *Anal Biochem* **1992**, 203, 173-9.
(36) John, M. B. *Biotechnol Appl Biochem*. **1999**, 30, 173-5.
(37)Matsuda, S.; Kodama, T.; Okada, N.; Okayama, K.; Honda, T.; Iida, T. *Infect Immun*, 78, 603-10.
(38) Tang, G.; Iida, T.; Yamamoto, K.; Honda, T. *FEMS Microbiol Lett* **1997**, 150, 289-96.
(39) Yangihara, I.; Nakahirs, K.; Yamane, T.; Kaieda, S.; Mayanagi, K.; Hamada, D.; Fukui, T.; Ohnishi, K.; Kajiyama, S.; Shimizu, T.; Sato, M.; Ikegami, T.; Honda, T.; Hashimoto, H. *J Biol Chem.* **2010**, 285, 16267-74.
(40) Song, L.; Hobaugh, M. R.; Shustak, C.; Cheley, S.; Bayley, H.; Gouaux, J. E. *Science* **1996**, 274, 1859-66.
(41) Hong, Q.; Gutierrez-Aguirre, I.; Barlic, A.; Malovrh, P.; Kristan, K.; Podlesek, Z.; Macek, P.; Turk, D.; Gonzalez-Manas, J. M.; Lakey, J. H.; Anderluh, G. *J Biol Chem* **2002**, 277, 41916-24.